High-precision control for Constant Distance Scanning Electrochemical Microscopy

Supervisors: Dr S. Baldi, Dr Y. Gonzalez Garcia

R.J. Noodelijk

Master of Science Thesis

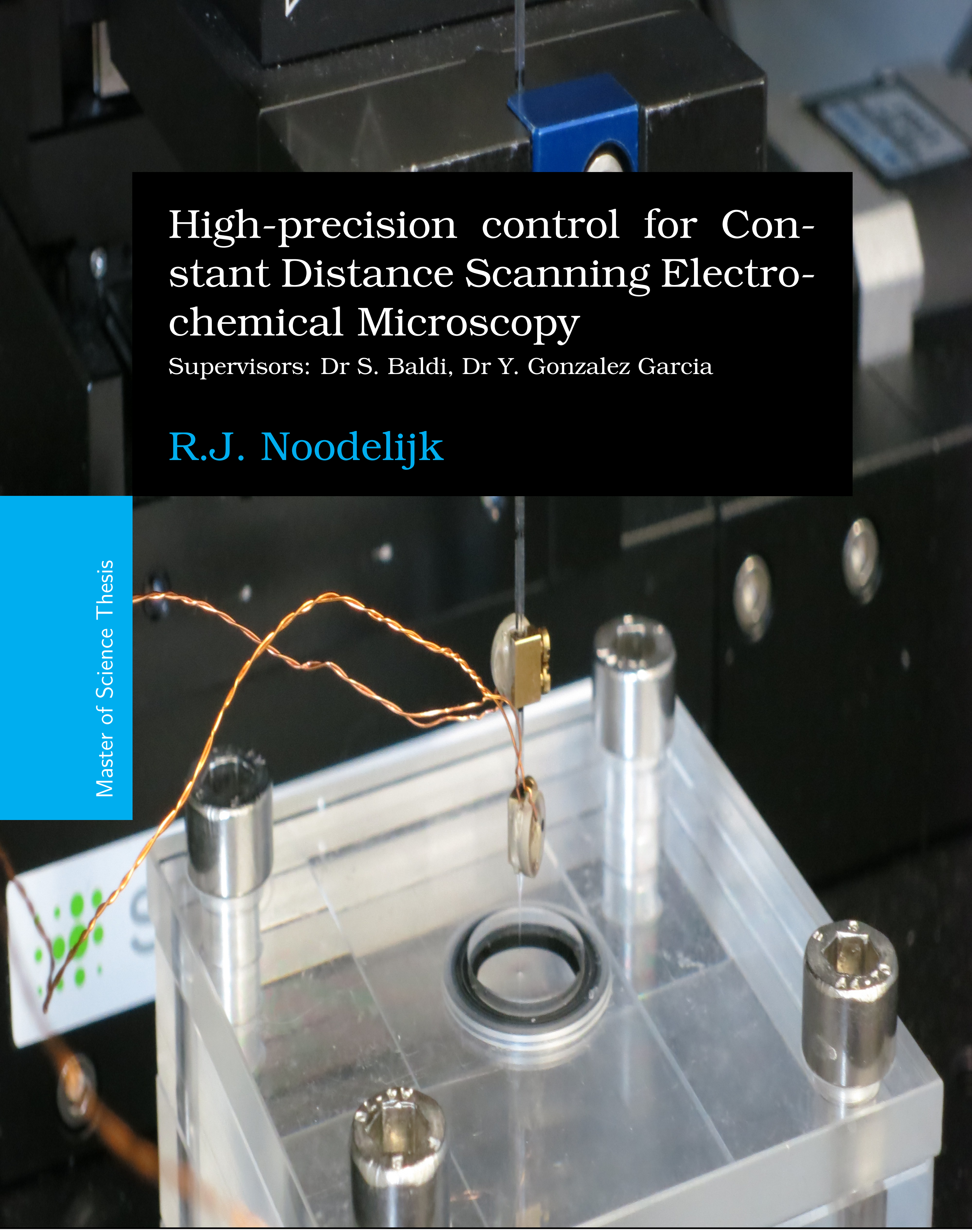

TU Delft Delft University of Technology

Delft Center for Systems and Control

High-precision control for Constant Distance Scanning Electrochemical Microscopy

Supervisors: Dr S. Baldi, Dr Y. Gonzalez Garcia

Master of Science Thesis

For the degree of Master of Science in Systems and Control at Delft University of Technology

R.J. Noodelijk

June 6, 2017

Faculty of Mechanical, Maritime and Materials Engineering (3mE) · Delft University of Technology

The work in this thesis was a cooperation between the Delft Center for Systems and Control (DCSC) and the Materials Sciences & Engineering deparment. Additional partial cooperation was offered by Sensolytics GmbH

Abstract

This Report covers the initial research into modeling the Scanning ElectroChemical Microscopy (SECM) system for the purposes of high precision control. The SECM system is a microscope based around electro-chemical effects. It operates in several modes relating on degrees of conductivity of the involved elements. The control is to be based on the observed additional damping the system experiences in control critical conditions. The improvement of this control is necessary to improve the precision and resolution of the system as well as gaining insight in its physical function.
Experiments where conducted using an industry setup of the system. This time with the system was used gather data important for model generation as well as requiring intuition on the intricacies of using the system and what type of precision can be used.
Next, mathematical descriptions are developed for all elements of the SECM system. First of the electrical components involved in the measurement and subsequently of the physics effecting the system. The approximations are picked with the goal of developing a state space model and maintaining a link to the physical world in its parameters. The most complex and relevant being the effect of hydrodynamic damping which is critical in the observed damping process.
It is modeled in the Lagrangian Energy approach, which captures only a part of the dynamics. Some additional factors are still missing. A departure from the homogeneous nature of the model is suggested. Experience with the system has led to increased insight into the systems behavior under various conditions and has provided a stepping stone towards more intricate future modeling attempts. While also providing inspiration for possible model free approaches.

Table of Contents

List of Figures

List of Tables

Chapter 1

Introduction

This Chapter will introduce the project and broadly outline the initial goals. To provide a proper context for the work some details of the shape and function of the Scanning Electro-Chemical Microscopy (SECM) device will be provided and finally a research question will be formulated.

1-1 Project Description

This research is a collaboration between the Delft Center for Systems and Control (DCSC) and Material Science Engineering (MSE) department of the TU Delft. The SECM system is a device already in wide use in the academic world for research purposes as well as industry applications. It was developed in Germany at the University of Bochum and further made ready for industry use at Sensolytic, a spin-off company also stationed in Bochum. The system is a microscope device that uses electro-chemical reactions to sense the distance to and properties of a surface at nano-precision. The system still has several challenges. One involves the fact that the device was never formally modeled and as such the approach to some of the control systems involved is fairly basic. A high quality model of the system will need to be constructed to control the distance to the surface d. The current method of control employed is relatively straight forward and inexact and as such a detailed model and sophisticated controller will allow for more precise control and resolution. Additionally it and the insight it provides serve as a stepping stone for tackling further challenges with the system.

This research has only just begun and this report is an initial look at modeling the SECM system in such a way that this control objective of a more accurate distance control, as well as possible future design refinements, might be achieved.

1-2 SECM System Description

The SECM is a member of the family of microscopes that Atomic Force Microscopy (AFM) systems are also a part of [5], [6], [7], [8]. It's functionality is based around electrochemical processes and how they effect the Faradaic current of an electrode immersed in solution near a surface. This allows the user to study the electro-chemical nature and processes near the surface. In practical terms it characterizes both the very exact distance to the substrate surface as well as it's properties, providing a detailed image of the surface. Depended on the type of material being investigated the SECM system can operate in several different modes, which makes it a versatile device.

1-2-1 SECM Set-up

The SECM device consists of an electrochemical cell, a potentiostat for measuring the current, a high precision positioning unit and a computer for processing the data.
The electrochemical cell or micro-electrode is essentially a glass tip containing a platinum conductor in it's core. This piece, from here-on out referred to as "the tip", is roughly 50-70 mm in long. It has a 1-2 mm diameter at it's base and at 10 mm from the end it quickly tappers down to as small as approximately 50 μm at the bottom, as seen in figure 1-1. This piece is hand crafted as will be described in later chapters and as such these dimensions may vary.
The positioning system is a high resolution 3 dimensional stepper motor positioning system, with a piezo stage for fine tuning the position. It provides precision upto one tenth of a nano-meter. It is a relative system though and will require a reference position. It can be seen in item A of figure 1-4.

1-2-2 SECM working principles

The system works by introducing the tip with the platinum electrode at its end into an electro-active species(the mediator). This will cause a diffusion layer in which the mediator M_{red} oxidizes into M_{ox} at the end of the tip. This will initiate a mass transfer to the tip itself which effects the measured current. The general function for this diffusion under the conditions as they are typically seen in the SECM system is seen in equation 1-1

$$i_{t=\infty} = 4nFCoDir \tag{1-1}$$

n is the number of electrons involved in the process, F is Faraday's constant, Di is the diffusion coefficient (cm^2s^2), Co is the concentration of the electro-active species ($mol \cdot cm^{-3}$) and r is the radius of the electrode. For the purposes of this research these are to be considered the relevant parameters that any alterations to the system for control purposes should not significantly effect.

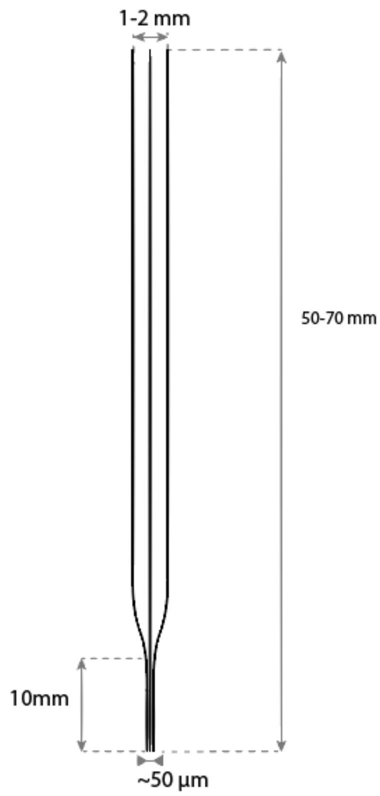

Figure 1-1: An illustration of the micro-electrode and relevant dimensions.

1-2-3 SECM Operational Modes

The system has several possible operational modes which are useful dependent on the conditions of the experiment, chiefly the type of substrate that is being investigated. The different SECM operational modes will be briefly discussed here [9].

Feedback Mode

The term feedback in this context isn't used in the control sense of creating a feedback loop for error correction. It is used more generally as a way to describe how 2 parameters interact. With a disk shaped electrode as described in the previous section the steady state current is governed by equation 1-1. When the tip approaches an insulating surface, it will interfere with the diffusion layer. Through this the layer will shrink and with it the current will drop. The current will eventually drop to 0 when the tip touches the insulating surface and the effect will be first seen at between 3 and 5 times the electrode diameter. Since there is an inverse relationship between the distance and the current this mode is referred to as negative feedback.
On the other hand if the surface approached is electrically active the surface will aid in the mass transfer by basically serving as an additional electrode. As such the current sensed will

increase once the electrode approaches the sample surface. This is commonly referred to as the positive feedback mode. Figure 1-2 shows the general idea of both positive and negative feedback in this context in action.

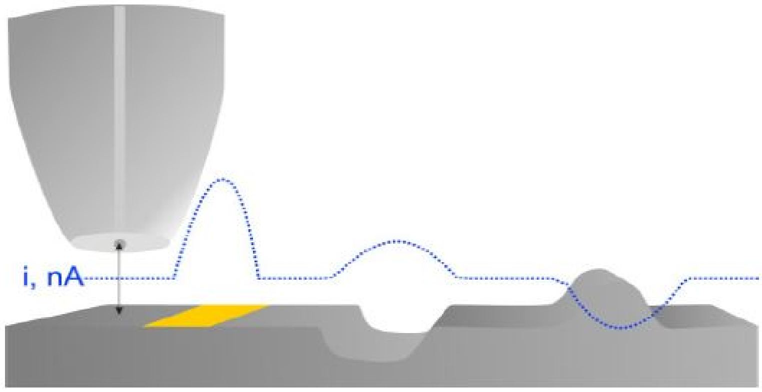

Figure 1-2: At a given height the output current is at a constant level for negative feedback. Once it crosses a electrically active surface the postive feedback kicks in and the current rises (the yellow area). Upon an indent the current rises and upon a hill it drops. For positive feedback this would be reversed. Source: [9]

Generator Collector Mode

Next the system is also able to work in what is called "Generator/Collector" mode. What this means is that there is no redox species in the medium and as such it is created at the generator and collected at the collector. Whether the electrode or the surface is the generator depends on where the current is applied. The current is fed through the generator. If the tip is the generator the mode is called TG/SC (Tip generator, Sample collector) and the reverse is called SG/TC mode (Sample generator, Tip collector). The advantage of these methods is generally seen in studying enzymes and other biological systems.

Direct SECM Mode

This mode turns the SECM tip into a spark abrasion device using electrical sparks to shape a nearby surface. This mode isn't very interesting for our purposes and it is assumed that one of the microscopy modes is the intended use unless otherwise mentioned.

1-3 Constant Distance Operation

During all of the mentioned operations the vital parameter in shaping the output is the exact distance between the micro-electrode and the surface. An important problem with the system is therefor that the it is unable to detect the difference between changes in topography and the phenomena it is intended to sense, such as differences in local electro-chemical activity. If the sample has ridges and levels of different height or if it is placed under a slight angle this

will cause unintended measurements. With the small distance between the electrode and the surface an additional issue is the risk of collision if the electrode is moved along the surface with a constant height.
For this reason it becomes important to ensure that the electrode is kept at a constant distance from the surface at all time, instead of keeping it at a constant height. Several approaches are suggested to achieve this goal. Some electrical methods were suggested using the innate system current measurements as source of feedback for control, but this work will not focus on these approaches. Instead it will look at the "Shear Force damping" approach.

1-3-1 Shear Force Constant Distance Control

This method is based on the observation that once the micro-electrode is agitated to vibrate lateral to the surface, forces on the tip will damp this vibration based on the distance from the surface. As such the difference between a measurement of the vibration and the applied excitation is a useful measure for feedback control of the height. Suggested sources of this damping force are only speculated at in literature and will be discussed in greater detail later in this report.
One such method is is seen in Scanning Near field Optical Microscopy, in which the vibration is read out by optical sensors. A disadvantage of this method is that an optical sensor will be difficult to position such that it is possible to move the electrode lateral to the surface and still have an accurate measurement. Figure 1-3 shows a representation of this system with the actuator and sensor piezo attached, representing the vibration as the forces in these piezo elements. Figure 1-4 shows a photo showing the full SECM setup in laboratory environment.
The method that is the focus of this research is the non optical method where the electrode is vibrated by a piezo plate and the measurement is performed by an identical piezo element. The difference between these signals is then fed through a Lock-In Amplifier (LIA) to find the damping. The current control method using this measurement is a simple proportional gain controller. It takes a set value for the damping initiated "error" that is experimentally found and corrects the electrode height once the measurements vary from this set value.

1-4 Aim of the Research

The aim of this research is to take a critical look at the method of constant distance control and try to improve it. For this purpose an attempt will be made to generate a model for the entire system. This includes modeling the dynamics of all the elements involved

The question that is intended to be answered in this research is:

"Is it possible to model the SECM system in such a way that positioning control can be improved, and with it the quality of acquired images?"

This is devided in a couple of sub questions that illustrate the aim of the research.

"Can a series of experiments be devised that will sufficiently show the required dynamic behavior of the system?"
"Is it possible to model the SECM system in an analytic manner?"
"Is it possible to clearly identify the systems real world parameters in the model?"
"Can a high precision constant distance controller be synthesized using the model?"

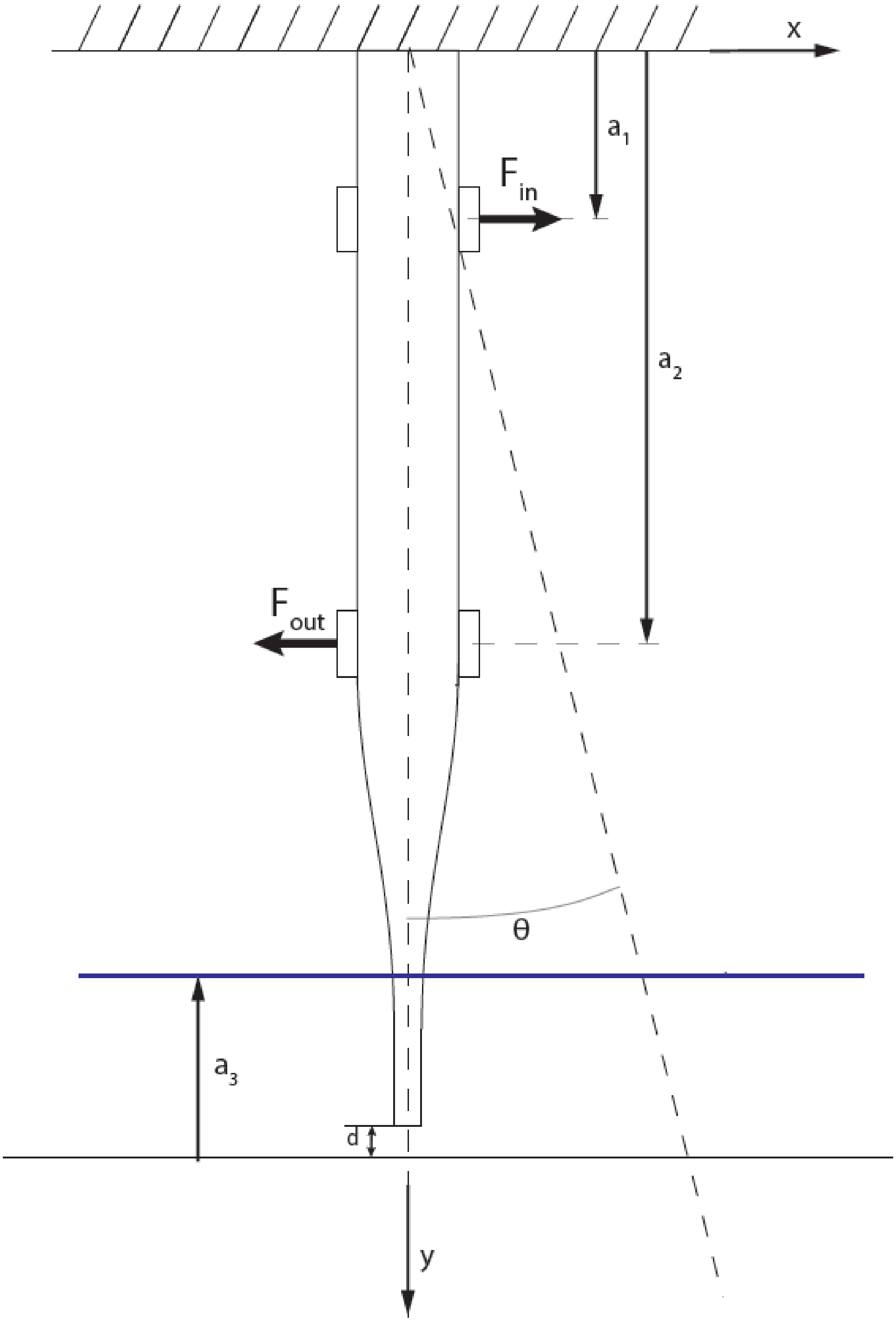

Figure 1-3: A schematic illustration of the micro-electrode as it is positioned near a surface. F_{in} and F_{out} represent the forces as they are applied by the piezo crystals as seen in figure 1-4 D and E. The a's represent the piezo positions and the height of the liquid layer, d is the distance between the tip and the surface and θ represents the micro electrodes angle of rotation in relation to the the clamped base.

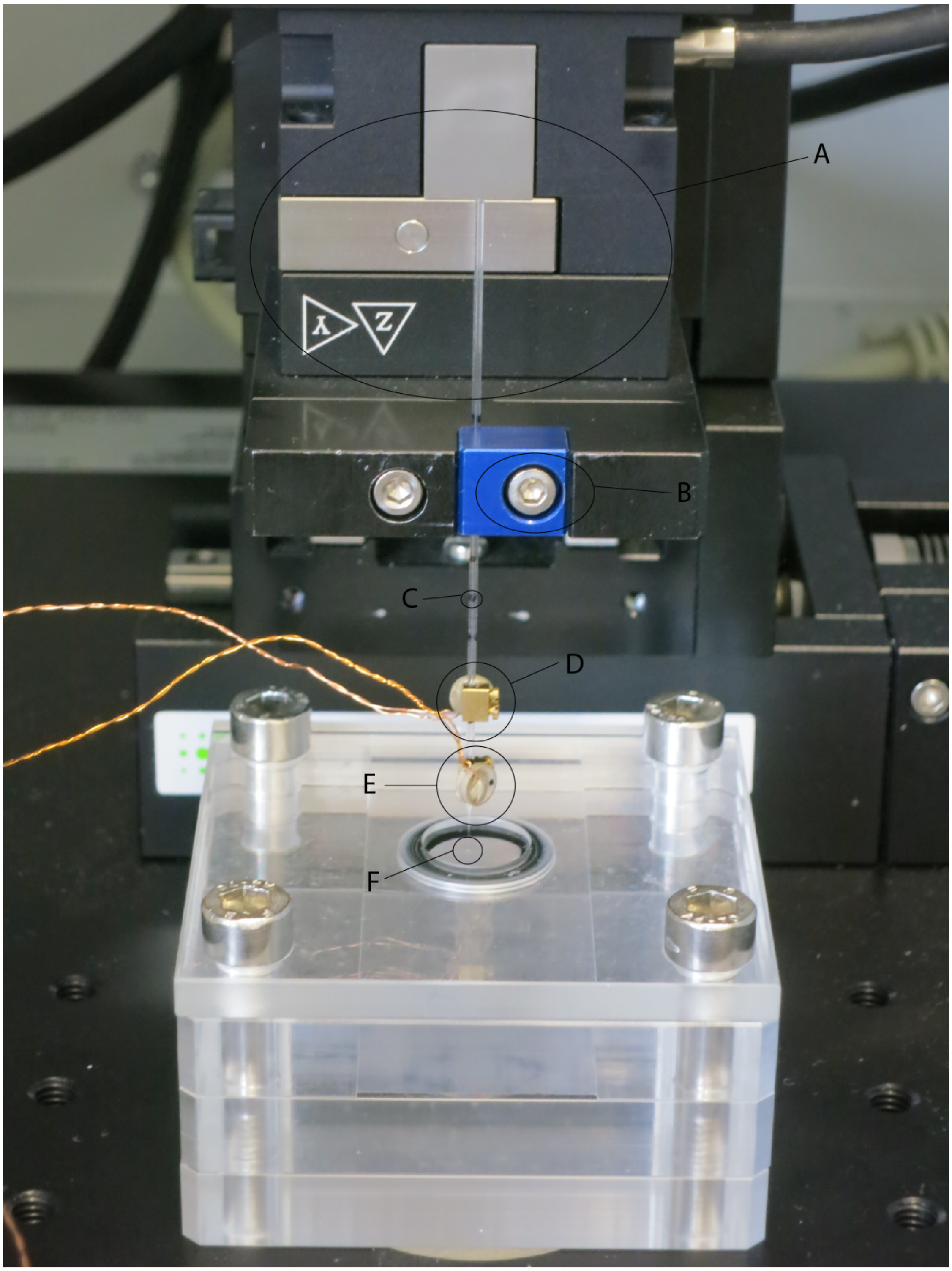

Figure 1-4: A detailed photograph of the SECM setup. A - The combination of stepper motor and piezo positioning system, B - The tightening screw to put the micro electrode in place, C - positioning markers for the piezo's at 5 mm intervals, D - The input piezo seen from the brass holder side with the tightning screws visible, E - The output piezo seen from the side of the piezo stack, F - The tip immersed in the liquid basin.

Chapter 2

Experimental Work

To generate data for testing and validating the model, a set of experiments was performed. For this purpose a session was planned at the production company of the SECM system, Sensolytic, situated in Bochum, Germany. This session was intended as an opportunity to generate data sets for the modeling work, but additionally it provided an opportunity for gaining insight and hands-on experience with the system.

2-1 Experiment Organization

First the structure of the experiments and the system hardware are discussed. This includes the types of experiments, required preparations and level of precision in experiment setup. First the types of experiments executed are discussed in detail, discussing how they are performed and what their purpose is. Next general preparation of the experiments and important assumptions and inaccuracies it brings with it are laid out. Finally the interesting aspects of the Scanning ElectroChemical Microscopy (SECM) system as used in experiments are summed up because they are important to keep in mind for discussion of the model.

2-1-1 Experiment Types

To gain some insight into the effect of several aspects of the behavior of the SECM system a number of variables was defined. The setup as it was used was not fully adjustable, the software was built for customer use and therefor provided only processed data necessary for microscope operation. Experimental detail was derived from within the context of these existing operations and there was little room for adjusting the code or introducing new sensors or actuators. With this in mind the following experiments where carried out:

1. **Frequency sweep**: This experiment ran the actuator through the relevant frequency range (100-400 kHz). The purpose is to find the degree of resonance at the sensor location by recording the average amplitude

2. **Approach Curve**: This experiment set the actuator frequency at a fixed value and then slowly reduced d (approaching the surface with the tip) and registered the average amplitude. Once the tip reaches the Shear Force (SF) range a sharp increase or decrease in amplitude is generally detected.

3. **Constant Frequency Excitation**: This experiment set the actuator at a constant frequency and simply recorded the sensor excitation at as high a sample frequency as possible. This experiment type required adjustments of the software because it was not a required test in normal use.

Within all these experiments the main variables that are used for testing are listed in table 2-1

Table 2-1: Variables for experimentation with SECM setup

variable	sensor position (mm)	sensor angle α (degrees)	Frequency (kHz)
range	0-25	20-90	100-400
step size	5	continuous	continuous

2-1-2 Experiment Preparation

To prepare for the experiments with the SECM setup, the same procedure has to be followed by a normal user of the system. This section shows the required procedures and their accuracy.

Preparation of the Micro-Electrode

First the tip needs to be prepared. The tip consists of a glass tube with a platinum wire inside and a tapered end. To make these tips, glass cylinders with platinum wires running through them, are divided in roughly 100 millimeter sections. These sections are then heat-treated and pulled in a specialized machine to form the tapered end. This also seals in the platinum wire.

Two different types of platinum wire diameter were available but only one type was selected for all electrodes. The quality of the electrodes selected was also strictly scrutinized in terms of straightness and damage as well as size of the glass to minimize trimming required to bring all dimensions within the same order of magnitude. This to keep the experimental results for different tips as similar as possible. Tips are very delicate and easy to damage so preparing several tips of similar dimensions and quality is wise.

The next step is to cut the tapered end to proper length. A microscope in combination with length marks on paper is used to guarantee precision. After the cutting of the tip the end is sanded down and polished to remove imperfections at the cutting edge as well as ensuring proper and predictable results of the damping in the shear force region. The procedure for this is to clamp the tip and lowering it towards a turntable with a mildly abrasive surface. The tip is rotated as well to ensure a level polish. A picture of a tip in the polishing station

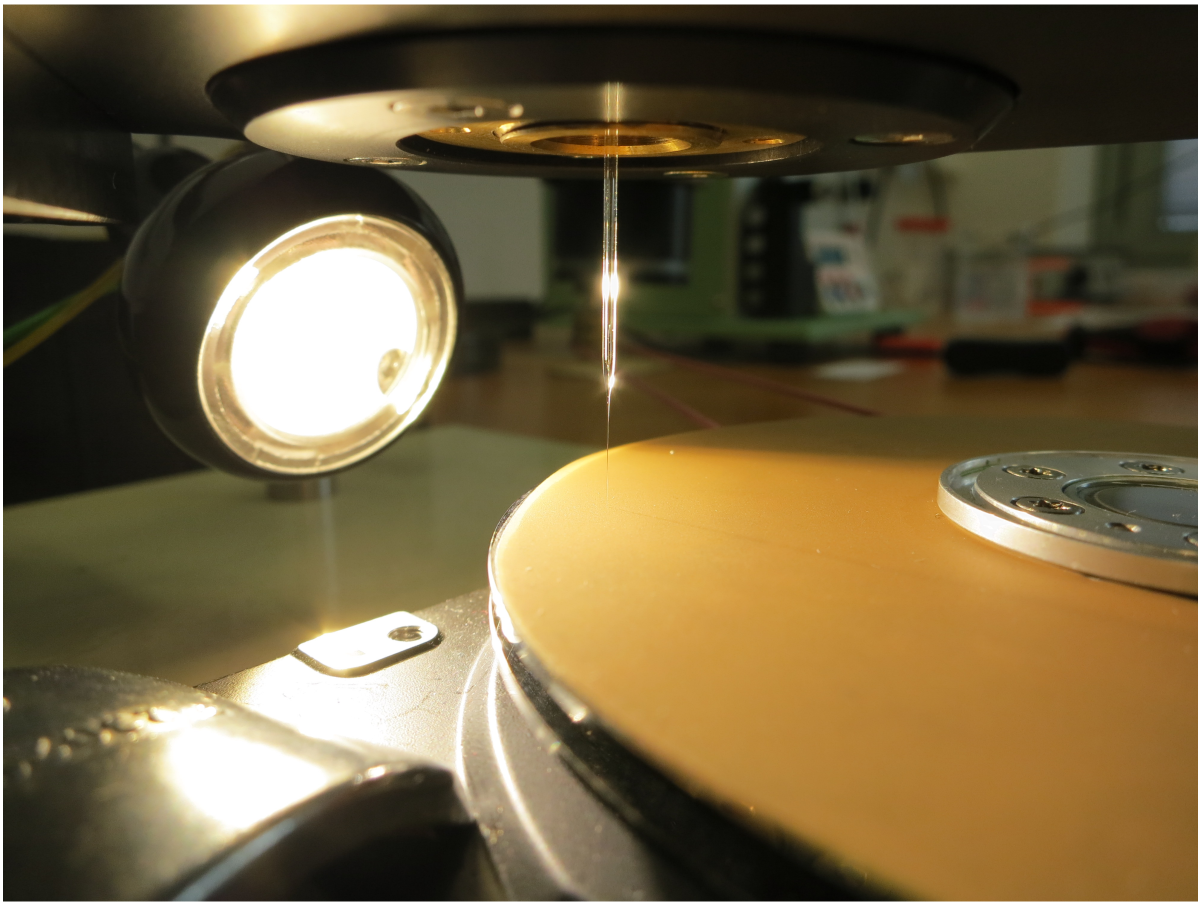

Figure 2-1: A high definition photograph of the polishing station, the light is shown because the shadows are the best way to detect whether or not your tip is touching the spinning surface below.

can be seen in figure 2-1

The final step is to inspect the tip under the microscope and to clean it in a bath of water that is made to vibrate to get rid of any dust or debris. Markings are then placed on the tip with a marker to indicate $5mm$ intervals for sensor and actuator placement. These markings start at the top of the tapered end.
A representative final product, including some dimensions, can be seen in figure 2-2 and 2-3

Tip Placement

Once a tip has been properly prepared, it will be placed in the SECM device. For this procedure, the sensors are slid onto the tip first. The brass holding the sensors has a small hole and a pair of tightening screws, they are individually slid across the tip and fastened at their required position and angle. The angle, as dictated by experience of the experts, is generally set at 45 degrees. Later experiments will be conducted to verify this value.

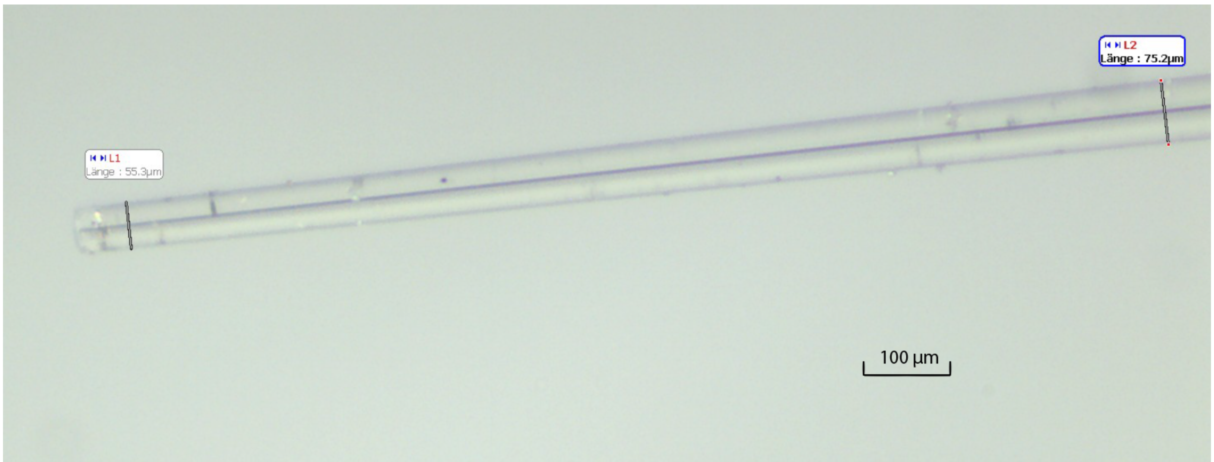

Figure 2-2: A microscopy image of one of the tips including some manually included size markers.

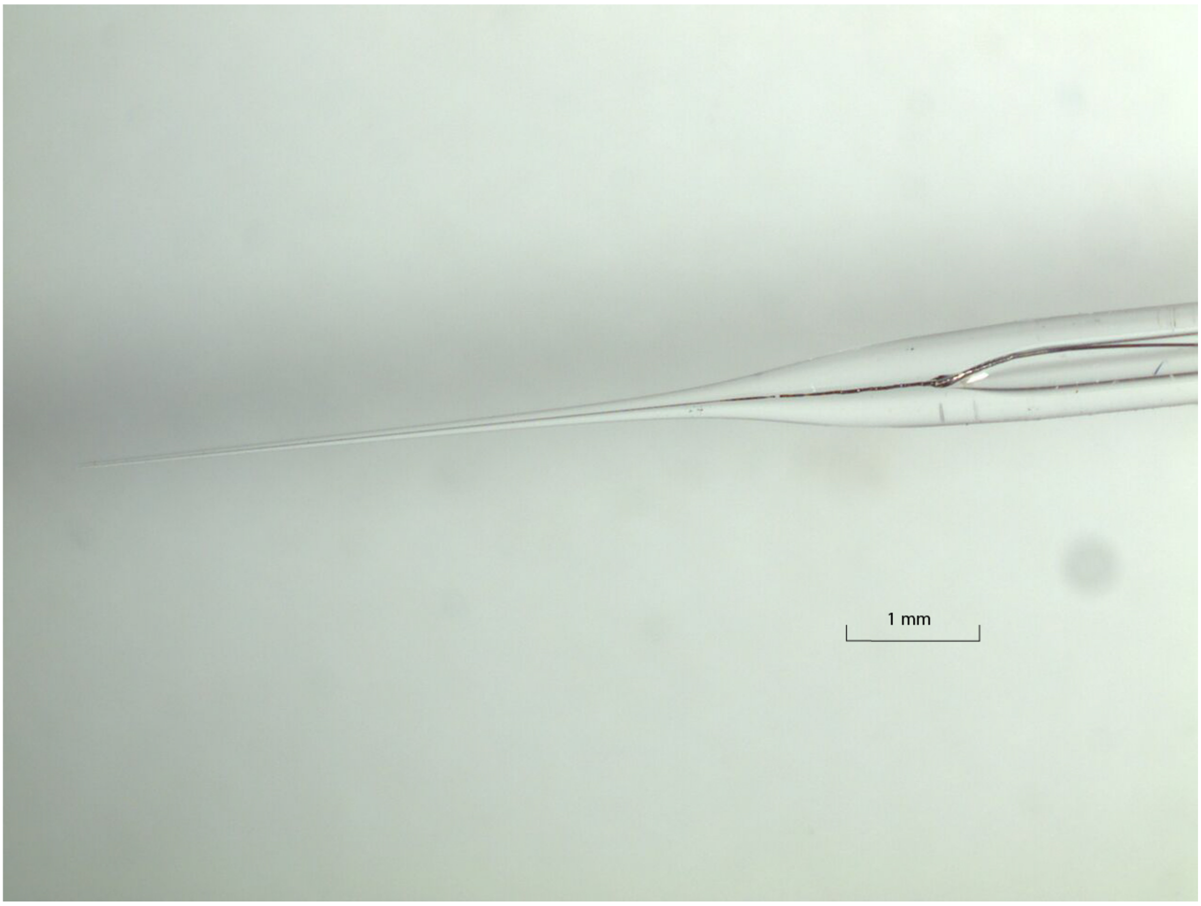

Figure 2-3: A slightly zoomed out picture showing the tip including the tapered end.

With the sensors placed and fastened, the tip is locked in by a magnetic clamp and then screwed tight. Special care is taken to position one of the sensors facing strictly forward to better judge the angle. There was no device in place to measure this angle, so it had to be judged by eye. Figure 2-4 shows a schematic view of what this will look like. Additionally, an inspection is preformed to ensure that non of the electrical wires attached to the sensors are causing short circuits.

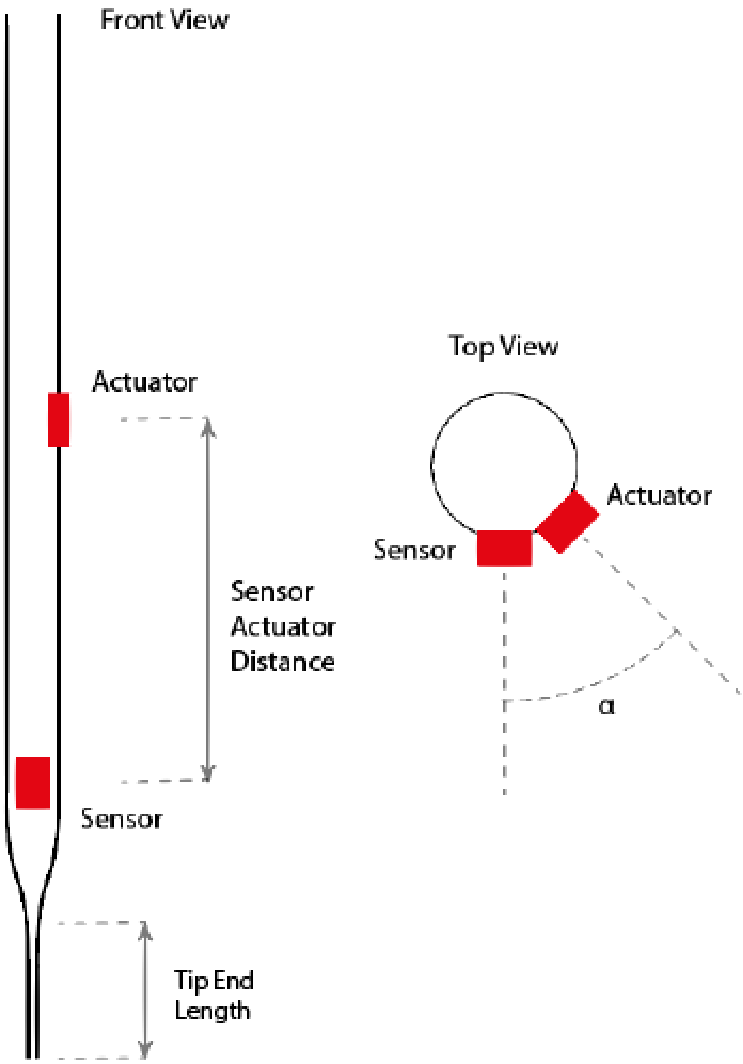

Figure 2-4: Shows a schematic front and top view of how the sensor and actuator are placed on the tip.

Cell Configuration

The liquid basin is a separate part that can be screwed onto the bottom plate. It consists of 2 plastic plates with the top plate containing a hole with a rubber ring lining the inside. A

Table 2-2: Positioning tolerances

sensor position (mm)	sensor angle α (degrees)
+/- 1	+/- 5

chemical pipet is then used to fill the cell with exactly 500ml of water.

2-1-3 Conditions and Assumptions

In terms of conditions, the experiment is as tightly controlled as possible under the applicable labs conditions.
The SECM system is placed in a Faradays cage to prevent outside electrical and radiation interference. All electrical wires are kept as short as possible. Where stripped, separation between wires is closely monitored to prevent any short circuits and keep leaking inductance at a minimum. The system is also placed on top of shock absorbent pads, to damp out environmental vibrations. It is still recommended to keep the table undisturbed during any experiments.

However, many of the factors are based on human perception and the skill of the operator. The angle and placement of the sensors are a clear example. Error tolerances are displayed in Table 2-2.

Additional factors that are harder to quantify are damages and the non homogeneous nature of the glass tip, caused by the fabrication procedure where heat treatment is involved as well as the cutting and polishing. Such imperfections could have a profound effect on the end result.

Based on experience, both simply handling the tip as it is moved from table to table to setup, as well as fastening the screws of the brass holders too tightly can easily cause damage which will influence the outcome of the experiment severely. Great care was taken to prevent such damages, but possible effect on the outcomes cannot be disregarded.

2-2 Experimentation Results

The results of the experiments are discussed here in the context of the experiments and the knowledge at that time. Additional conclusions and insights gained by comparing the experiments to the model and control attempts will be discussed in later chapters.

2-2-1 Frequency Sweep

In total about 20 sweeps were carried throughout the week, including repeated runs. A number of separate graphs are shown in appendix A and an example of a typical graph is provided in figure 2-5.

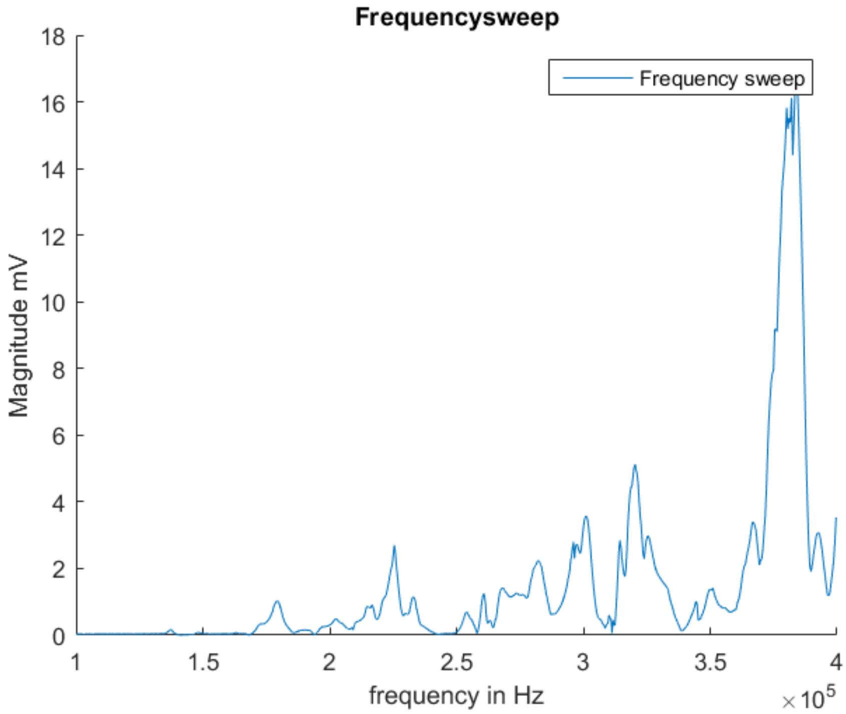

Figure 2-5: A typical frequency sweep response. With the frequencies ranging from 100 kHz to 400 kHz it shows 5 sample average of the absolute amplitude measurement

All frequency sweep experiments show very similar behavior: a gradually increasing amplitude for increasing frequencies. They show relatively noisy, but clearly distinct peaks. The example in figure 2-5 shows peaks at 175, 225, 300, 325 and 375 kHz. It could be argued that the peaks around 300 kHz are the result of the same resonance peak.
The final peak between 350 and 400 peak is always dominant, regardless of tip or conditions (in air or liquid). And repeated experiments on the same tip under the same conditions return almost identical graphs as seen in figure 2-6. The changes that do occur are in noise behavior between peaks and sharp edges. Where one run shows a rising line, repeat experiments sometimes show additional local spikes but never significant enough to suggest different dynamic behavior. However, very small changes to the setup do change the graph raising and lowering it a bit, slightly re positioning the sensors or even the wires. The wires are relatively stiff and they might put a very slight strain on the tip.

Finally, a comparison is drawn between a frequency sweep in the bulk and a sweep in the SF region, the relevant graph is seen in figure 2-8. Observable is a significant change in behavior around several of the peaks, with the most dramatic being around the dominant high frequency peak. This behavior does however appear to be highly unpredictable. Sometimes the peaks are higher and other times they are lower. However, throughout multiple experiments the behavior where the dominant peak is lowered seems most prevalent. This does raise the question what type of dynamic would cause such effects. Initial suggestions are the different vibration modes of the system being effected by the system differently. Either because of damping or because the system starts to behave as if the end point is clamped once the shear force starts to take hold. A picture illustrating this difference is shown in figure 2-7 This

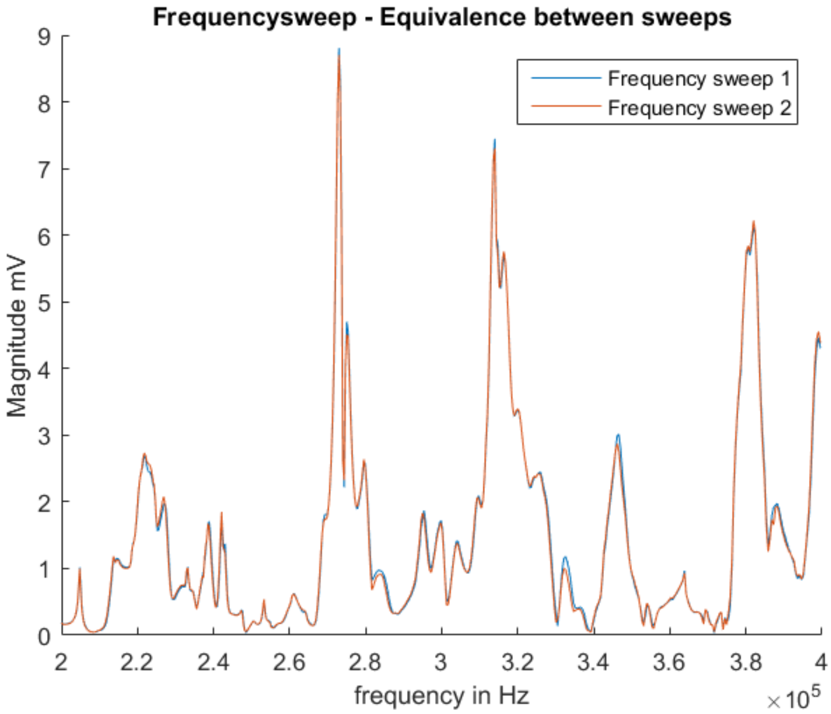

Figure 2-6: A comparison between two experiments preformed under identical conditions. Showing the high degree of similarity between two such experiments in the entire frequency range.

remains a relevant question however that any model of the shear force damping should strive to represent.

2-2-2 Approach Curve

The approach curve is used in the industry to find the location of the shear force region in terms of x. The x height of the tip depends on the size of the tip, the point of clamping as well as the manual adjustments of the positioning motors. Therefore, the position is completely relative and finding an absolute value is not possible. However, once the tip touches the surfaces the approach plot flattens out and as such an absolute value for the x position is set. The approach is discrete, and the step size can be set manually. Most of the time a step between 1 an 0.1 μm is taken to ensure speed but the smallest step the positioning piezo is able to handle is 2.5 nm. Below 2.5 nm the positioning piezo doesn't reach the threshold to start movement and the tip doesn't move while a change in position is registered digitally. Approach curves either increase or decrease upon reaching the SF region depending on the effect of the SF on the frequency sweep at that frequency.

A large number of approach curves was provided, they can be either a step up or down in amplitude, an example for both is provided in figure 2-9 and 2-10.

Finally an attempt with the smallest possible step was taken, at 2.5 nm shown in figure 2-11. This picture is displayed very large to allow for closer inspection of the details.

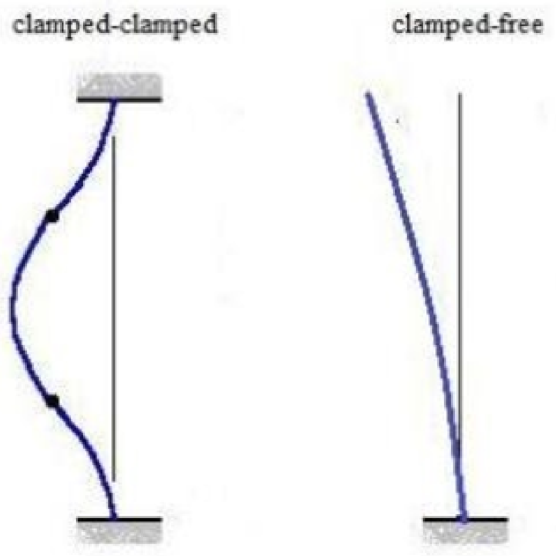

Figure 2-7: A clamped clamped been excitation on the left, and a clamped free excitation on the right. Showing the large differences in amplitude likely to occur on various places along the beam for similar excitation. source: https://sites.google.com/site/kolukulasivasrinivas/matlab-fea/beam-finite-elements/natural-frequencies-buckling

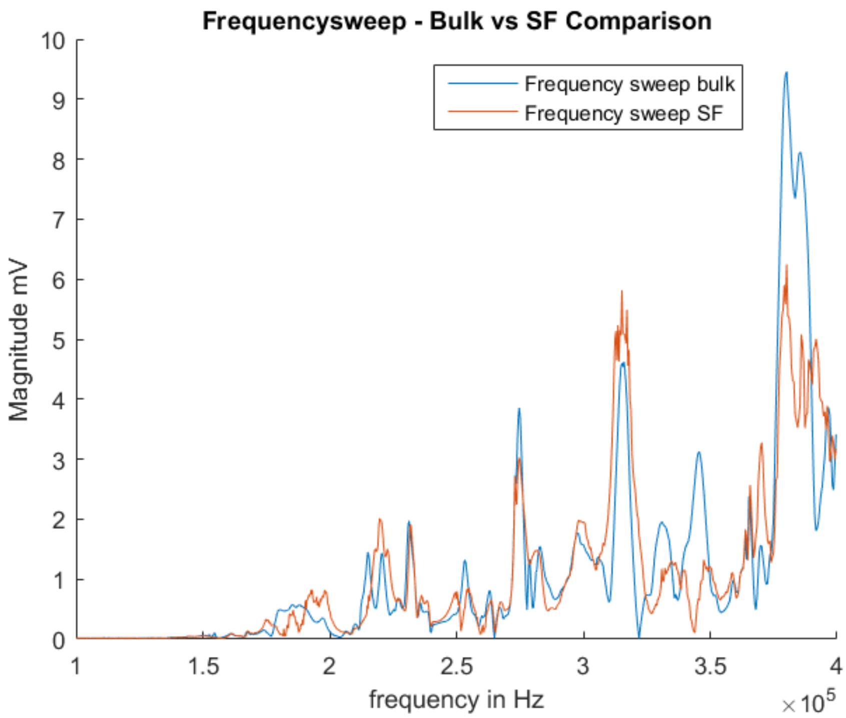

Figure 2-8: A comparison between the frequency sweep in the bulk(blue) and near the surface in the SF region(red).

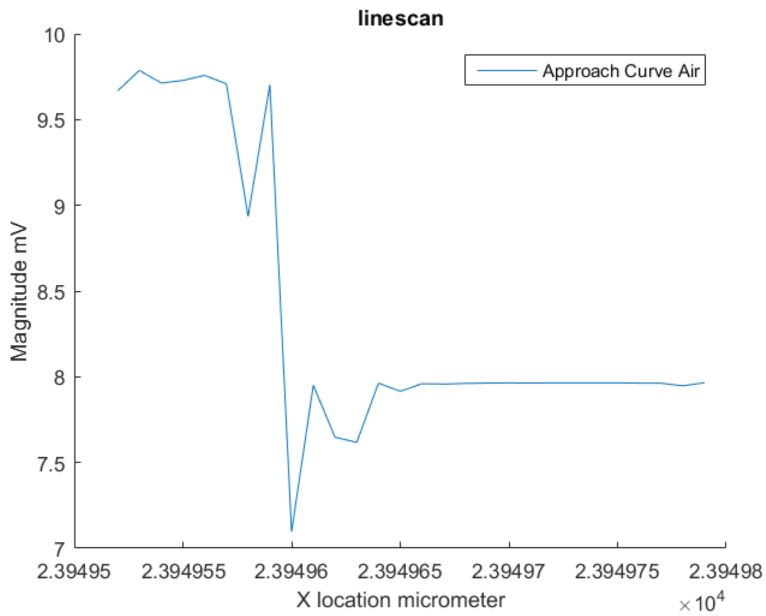

Figure 2-9: An approach curve starting at a low value and jumping to a higher value. Notice the heavy noise at the start and the end of the jump.

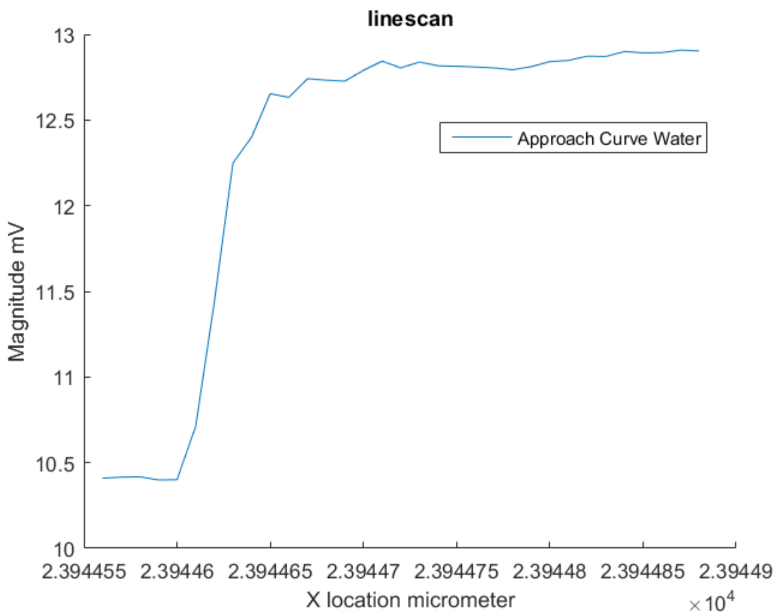

Figure 2-10: This figure shows an approach curve starting at a high value and jumping to a lower value. Notice that for this run the curve is much smoother.

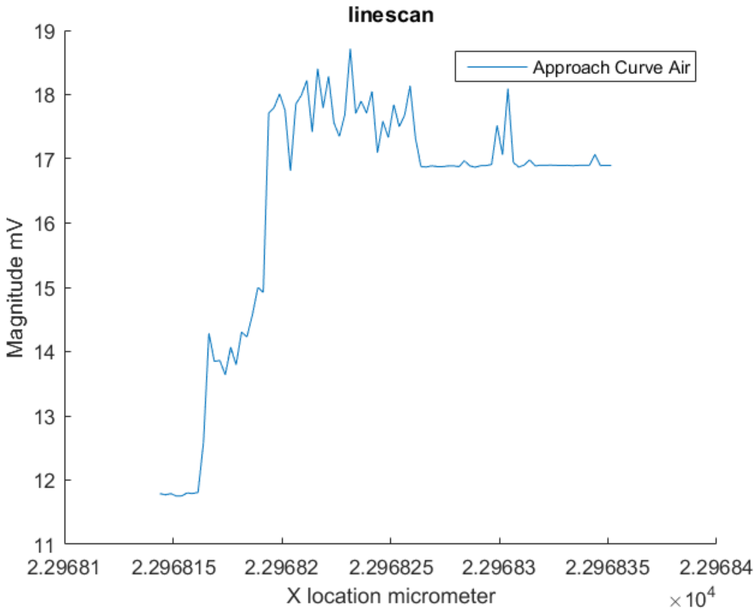

Figure 2-11: This figure shows an approach curve starting at a low value and jumping to a higher value. Notice the heavy noise at the start and the end of the jump.

All of these show a very similar response. Upon entering the SF region the response starts to increase or decrease respectively at a slow rate which exponentially increases with the distance. When the tip reaches the surface the response abruptly levels out to a new constant amplitude value. All experiments showed this behavior, sometimes there was some apparent initial inverse response and often there was varying amounts of noise. This could often be significantly reduced upon repeated experiments. On a lower sampling right it might conceivably be possible to map these responses to a general function fairly accurately which could prove a useful tool for control.

Constant Frequency Excitation

This set of experiments was intended to generate rich excitation data to allow for possible identification of the dynamics as well as having an additional metric, on top of the frequency sweep, to test simulation results with. The result of a run at 100 kHz is shown in figure 2-12 which already shows a problem quite clearly. Strange peaks of almost equal height show up in the behavior. After discussion no satisfactory explanation was found for this behavior but it is obvious that the experiment is severely under sampled at 20 kHz, the highest possible sampling frequency in the available setup. This is suggested as the primary reason for the erratic behavior. The zoomed in plot in figure 2-13 shows that the band in figure 2-12 displays at least the type of behavior one would expect from a multi-mode vibration. However, there is no discernible section in this sample where some kind of cyclical steady state is seen. One would expect a cyclical pattern for a constant harmonic input. None such pattern appears in a reasonable time window considering the excitation frequency.

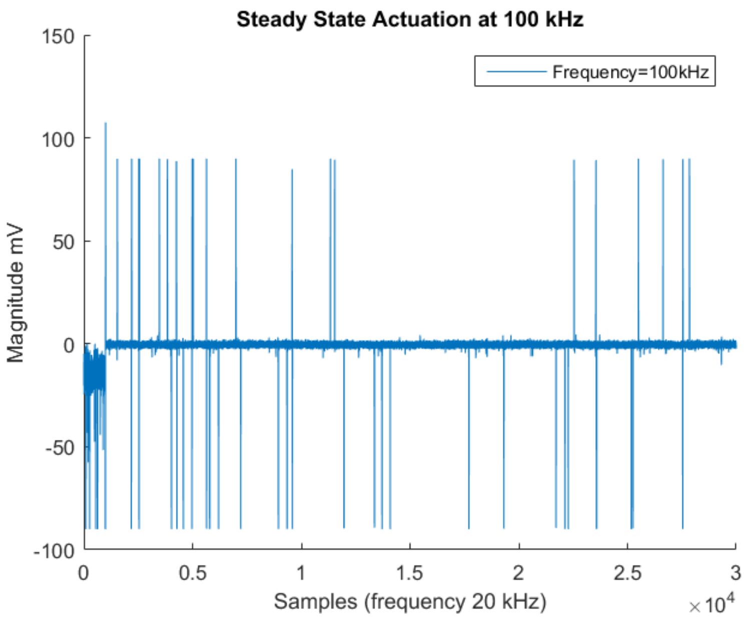

Figure 2-12: Constant actuation at 100 kHz, sampled at 20 kHz. Spikes in behavior are difficult to explain but are in all likelihood caused by severe under sampling.

In figure 2-14 the 250 kHz actuation case is shown, and the problems appear identical to those in the 100 kHz case of figure 2-12. The spikes are also constant, although they are not of equal height to the previous case. The zoom in of this graph at figure 2-15 however shows the sampling issues even more clearly. It becomes readily apparent that the setup as it was used in Bochum was not equipped to carry out this type of experiment and unfortunately the results of these experiments will have to be disregarded for the purposes of modeling.

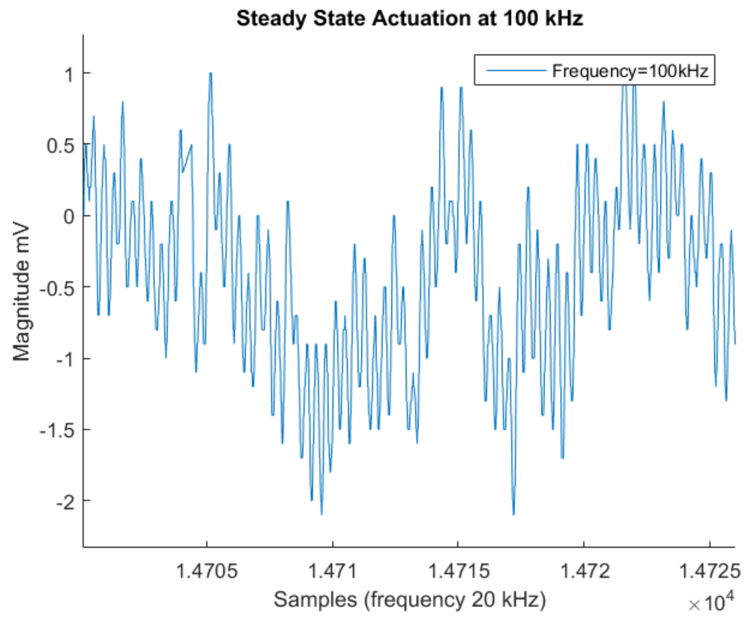

Figure 2-13: A zoomed in view of the 100 kHz plot, show behavior along the lines of what was expected, but much more chaotic then would seem likely at constant sinusoidal actuation.

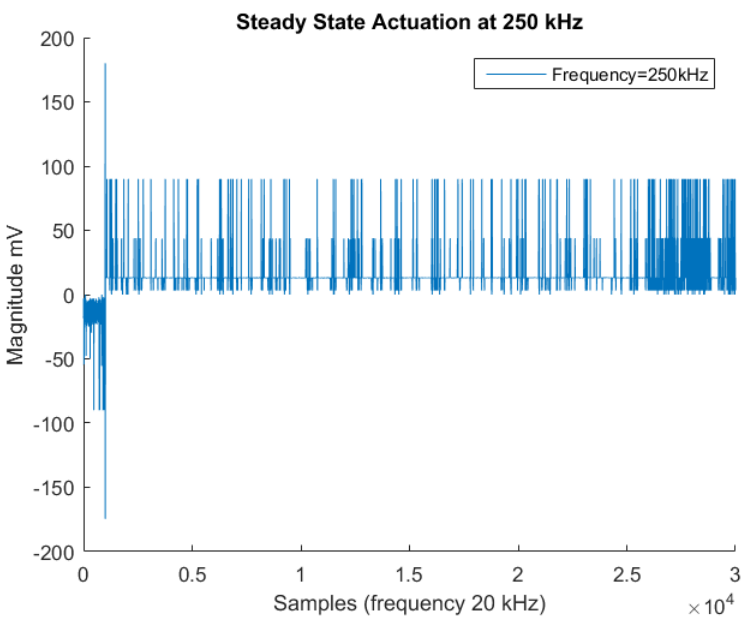

Figure 2-14: Constant actuation at 250 kHz, sampled at 20 kHz. Similar issues appear as in the 100kHz case of fig 2-12.

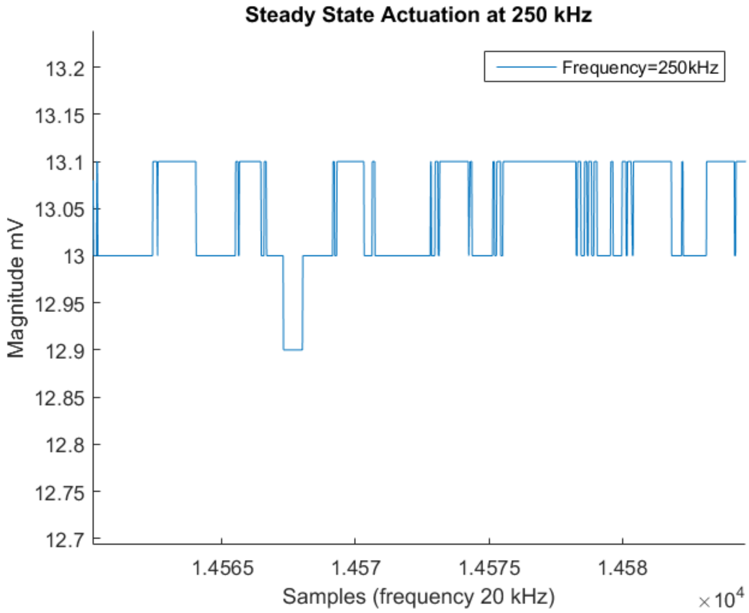

Figure 2-15: A zoomed in view of the 100 kHz plot, show behavior along the lines of what was expected, but much more chaotic then would seem likely at constant sinusoidal actuation.

2-3 Discussion

The experimental work has provided a significant body of data for evaluating and modeling the system. Especially the data based on the existing functionality of the device, such as the frequency sweep and the approach curve, have provided a robust set of runs that should give a very good idea of the way the system behaves for different excitation frequencies. Additionally it has provided insight into the details and peculiarities that have to be taken into account once the system is used in practice rather then based on the theory alone. It has shown that the hand crafted nature and assembly of the device is an important factor in some of the differences that occur between different experiments.

Chapter 3

Analytical Model Theory

This chapter will discuss the analytical model choices made to represent all the element of the Scanning ElectroChemical Microscopy (SECM) system. Detailing how the physical phenomena involved might be analytically modeled. It looks at first at the dynamics of the overall system, the micro-electrode tip and all it's elements, and how they can be modeled analytically. Secondly, details of individual elements are discussed and how they come together in a final model description.

3-1 Analytic Method

An Analytic modeling method had to be selected to serve as the basis for MATLAB simulation and an eventual controller. To be able to generate a model, all the aspects of the system vital to the relevant behavior, behavior important for the eventual controller, need to be included. The following elements need to be included in any model to reach this goal:

1. A main body of the tip with enough flexibility to capture high frequency behavior. From literature it shows that for a beam of the dimensions involved and the frequency range employed in SECM operation, a large number of vibration modes are relevant. Comparable Atomic Force Microscopy (AFM) systems show upto 8 active modes. With this in mind a more rigid system will likely cause problems.

2. The masses associated with the sensor and actuator and their brass holders.

3. A term or terms associated with the damping associated with the "Shear Force region" effect which can be expressed in terms of the distance between the tip and the substrate surface.

A model that contains these elements should proof useful to investigate the behavior of the system and how it changes with each of the relevant physical properties. The manufacture of the tips as well as sensor placement is done by hand. This means that a lot of variables will change from setup to setup. Once the effect of such properties (such as stiffness and various damping factors) can be identified as a particular difference in the models output, a change in in the measurements might be attributed to a change in one of these properties (due to damage, different placements or conditions). And as such fit the model without needing to fit it to the model entirely blind.

3-1-1 Black Box Identification

As stated before the system for which the model is build will vary in properties from one situation to another. Additionally, the manufacturer of the device has a particular interest in the physical properties and behaviors of the system at a more detailed level then are currently available. This to allow the manufacturer to show more knowledge of the system and how it behaves in communication with customers.
Consequentially a block box identification approach, while initially seeming to be a reasonable approach for a system with this complexity, is not preferable. This type of model lacks any connection to the physical properties of the system and as such gives no insight into the variations in the systems behavior as a function of changing properties. Therefor the model would loose it's function as a demonstration tool since large analytic functions without identifiable elements are unappealing to anyone not familiar with system modeling. More importantly it will be very hard to adjust the model by hand after conditions or properties change. Very likely changes which would warrant such changes is the replacement of a micro-electrode or even the system being left alone for an extended period of time allowing it to set and pre-existing tensions to release and possibly even cause gradual damage. Such damage has been seen to change the output of the system significantly in the experimental environment.
With this in mind a black box identification would have to be repeated at every significant change in the SECM system. This would be time consuming and not user friendly. For this reason it is not considered as a modeling approach at this stage. It should be noted that a grey box identification of a number of parameters defined by physical properties of the system is a likely approach to fine tuning any eventual modeling solution.

With this in mind a reasonable place to start looking is a continuous modeling approach.

3-1-2 Continuous Approach

For a continuous approach the system is evaluated as a beam upon which a shear force is applied to cause the displacements. For shear force the energy equation based on Newton's equations equals:

$$-(V + dV) + f(x,t)dx + V = \rho A(x)dx \frac{\partial^2 w}{\partial t^2}(x,t) \tag{3-1}$$

This eventually reduces to

$$EI\frac{\partial^4 w}{\partial x^4}(x,t) + \rho A\frac{\partial^2 w}{\partial t^2}(x,t) = f(x,t) \tag{3-2}$$

with $f(x,t)$ the external force, E the Youngs modulus, I the moment of inertia, ρ the density and A the cross section of the beam.

Notice that for this approach there is an assumption of a homogeneous beam. In order to introduce the added masses and the geometry of the tip both I and A become x depended and the whole thing becomes very difficult to solve. Additionally you loose all feeling for what these things mean in the solution. An x variable cross section doesn't provide insight on the effect of a slightly larger mass or a different mass position. Hence the whole equation would have to be newly evaluated every time a new tip is introduced or the conditions change.

Rayleigh's Method

A second approach is to look at Rayleigh's Method to find the fundamental frequencies. This method is much easier to evaluate and uses kinetic and potential energy to find the equations of motion.
For a beam the kinetic energy of the beam can be evaluated as:

$$T = \frac{1}{2}\int_0^l \dot{w}^2 dm = \frac{1}{2}\int_0^l \dot{w}^2 \rho A(x)dx \tag{3-3}$$

and the maximum value of this energy amounts to T_{max} equals

$$T_{max} = \frac{w^2}{2}\int_0^l \rho A(x)W^2(x)dx \tag{3-4}$$

with W the maximum deflection of the beam. For Potential energy we find

$$V = \frac{1}{2}\int_0^l M d\theta \tag{3-5}$$

Substituting for bending moment M and angle θ

$$V = \frac{1}{2}\int_0^l \left(EI\frac{\partial^2 w}{\partial x^2}\right)\frac{\partial^2 w}{\partial x^2}dx = \frac{1}{2}\int_0^l \left(EI\frac{\partial^2 w}{\partial x^2}\right)^2 dx \tag{3-6}$$

and in similar fashion to the kinetic energy we find the maximum value V_{max}

$$V_{max} = \frac{1}{2}\int_0^l \left(EI\frac{d^2 W(x)}{\partial x^2}\right)^2 dx \tag{3-7}$$

The frequency dependend Rayleigh's quotient is found by taking

$$R(\omega) = \frac{V_{max}}{T_{max}} \tag{3-8}$$

While this method is simpler and eliminates the partial differential form the equations, it only provides the natural frequencies and isn't enough for simulation. Having concluded this, a more discrete approach will be required. However, the insight given by Rayleigh's Method suggests an energy based approach.

3-1-3 Discrete Lagrangian Approach

A discrete approach might be more suitable for creating an analytic model while still allowing for online simulation and is therefore useful as an observer or the basis for a state feedback type control system.

If a discrete system is defined, one approach would be to simply build up the newton equations for each individual discrete element of the system. This is relatively simple for small systems but once the systems become more complex and there are added elements setting up these equations becomes very complex. For these systems a simplification is preferable. One such method is the Lagrangian Energy method. It's a method based around a balance of the kinetic and potential energies with the external forces in the framework of the smallest amount of required generalized coordinates.

Generalized Coordinates

Generalized coordinates are that minimal set of coordinates required to completely model the system. They appear because of constraints on the system, for example in the case of a pendulum the end point moves through the 2 dimensional plane in the x_1 and x_2 direction. However, it is fairly simple to map both unto the angle of rotation θ. as seen in equation 3-9 and 3-10 in relation to the system of figure 3-1.

$$\xi_{11} = l_1 \cos\theta_1 \tag{3-9}$$

$$\xi_{21} = l_1 \sin\theta_1 \tag{3-10}$$

Any part of the energy introduced will then automatically be written in terms of θ.

Energies and Lagrangian equations

The next part is to take the generalized coordinates and express all energies in the system in terms of the generalized coordinates. There are 3 types of energies that can be identified for this purpose.

1. Potential Energies: Potential energy is energy possessed by a body by virtue of its position relative to others, stresses within itself, electric charge, and other factors.
2. Kinetic Energies: The Kinetic energy of an object is the energy that it possesses due to its motion.

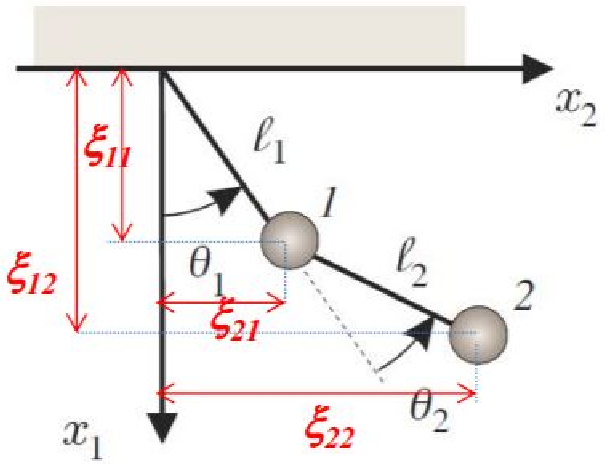

Figure 3-1: A double pendulum, ξ_{11} and ξ_{21} are to be mapped unto θ_1

3. Non Conservative forces: these forces are those that don't apply in the above categories. A clear example relevant to this research is the energy of a damper.

The Lagrangian approach is derived from the d'Alambert equations with the newton equations expressed on a virtual displacement

$$\sum_{k=1}^{N}\sum_{i=1}^{3}(m_k \ddot{u}_{ik} - X_{ik})\frac{\partial u_{ik}}{\partial q_s} \tag{3-11}$$

and rewriting them in terms of energy to eventually find

$$\frac{d}{dt}\left(\frac{\partial T}{\partial \dot{q}_x}\right) - \frac{\partial T}{\partial q_s} + \frac{\partial V}{\partial q_s} = Q_s^{ncons} + F_{ext} \tag{3-12}$$

including the generalized coordinates q and the external force F_{ext}.

3-2 Modeling considerations for the SECM system

If an attempt is to be made to model the SECM system within the suggested Lagrangian framework, all of it's relevant elements will have to represented in a uniform way such they can be combined into one model. Different physical phenomena and system elements will all have an effect on the dynamics of the system and it's output system. Assumptions and approximations will have to be made for all of them in order to unify them into one model that is able to predict the systems behavior as a whole. Due to the nature of the method, the goal is to represent all of these elements in terms of point masses, springs and dampers. This section will look at the entire system and seek to describe it in this manner.

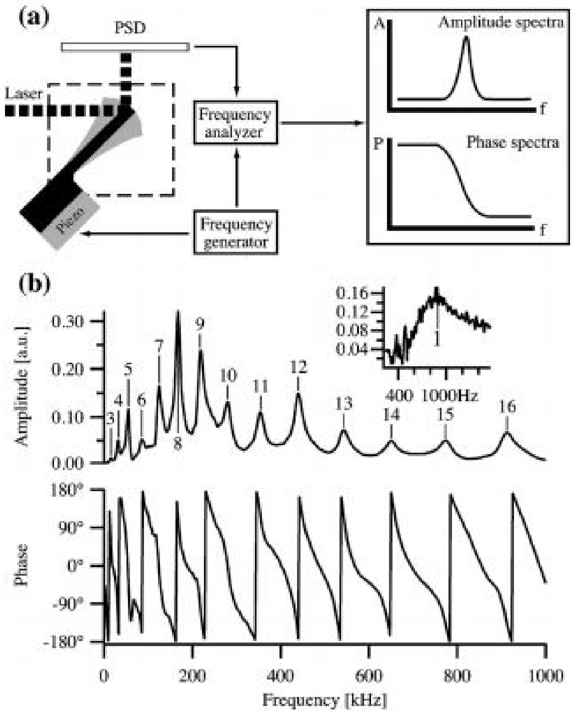

Figure 3-2: Illustration showing the frequency spectrum of a vibrating micro cantilever beam. a) provides the setup for the used experiments, a cantilever under a 45 degree angle excited by a piezo crystal is read out by a laser b) Showing a bode plot revealing a range of resonance peaks associated with various vibration modes. source: [1]

Discretization of the Tip

To model the tip using the discrete Lagrangian approach the tip must be discretized [11] [12]. A basic method of discretizing a beam is by modeling as a rigid beam connected to the base by a spring. Under this theory the beam will be characterized by equation 3-13.

$$k_{eq} = 3EI/L^3 \tag{3-13}$$

This model is still very basic, and isn't very likely to meet the general requirements as set out in 4-1. Previous work on the SECM system and similar AFM systems suggest that these tips behave under a large number of vibrational modes. This work suggests modes upto the 8^{th} are relevant for this purpose.

To allow the creation of a MATLAB model by the Lagrangian energy approach suggested above, inspiration is taken from Finite Element Modeling (FEM) approaches and the cantilever beam is divided up into a large number of connected segments, each connected with it's neighbors by a spring with the constant as defined in equation 3-13 with L the segment length. Basically turning into the type of system displayed in figure 3-1 but with much more segments and an introduced mass for each segment as well as a spring at the base. A possible addition is to also introduce a damper for each segment to give more freedom to effect the behavior.

All this will allow a lot of freedom of movement for the model while still having a discrete model that can be used in a State Space type model.

Finally dampers will likely be needed to model the behavior more realistically Added damping effects are modeled under the assumption of a simple viscous damping model This causes the damping energy for purposes of the Lagrangian approach to system modeling to be equal to [13]:

$$R_{nc} = 0.5 \left(\sum_{i=1}^{2} c \cdot \dot{x}^2 \right) \tag{3-14}$$

with the damping coefficient c and the velocity $\dot{x}$.

Number of Segments

The number of segments required to properly capture the behavior of the beam depends on dominant mode to be investigated. looking at picture 3-3 a pattern emerges in the higher modes of vibration. the first mode can be characterized by 1 segment. If we keep all segments of equal length the second requires 2 going up, 2 going down back to zero and then 1 at the end. For the 3^{th} mode this same approach gives 9 segments. Continuing this pattern for higher modes see table 3-1.

mode	1	2	3	4	5	6	7	8
# segments	1	5	9	13	17	21	25	29

Table 3-1: Number of segments to describe dynamic behavior

3-2-1 Sources of Damping

The most important factor in the dynamics modeling lies in attempting to explain the effects responsible for the damping. The relevant aspects have to be selected and then approximations have to be made to model these effects with the mass/spring/damper elements.

Van der Waals Forces

The first suggestion for these forces lies in the Van der Waals force attraction that objects feel once they are brought within close proximity of each other. The physics of this will not be described in great detail but a summary is that once two molecules approach each other a force is observed between these molecules. For objects this force becomes relevant once they approach each other close enough that the molecules at each surface will begin to exact an attractive force upon each other. While this force will always be present it has to be

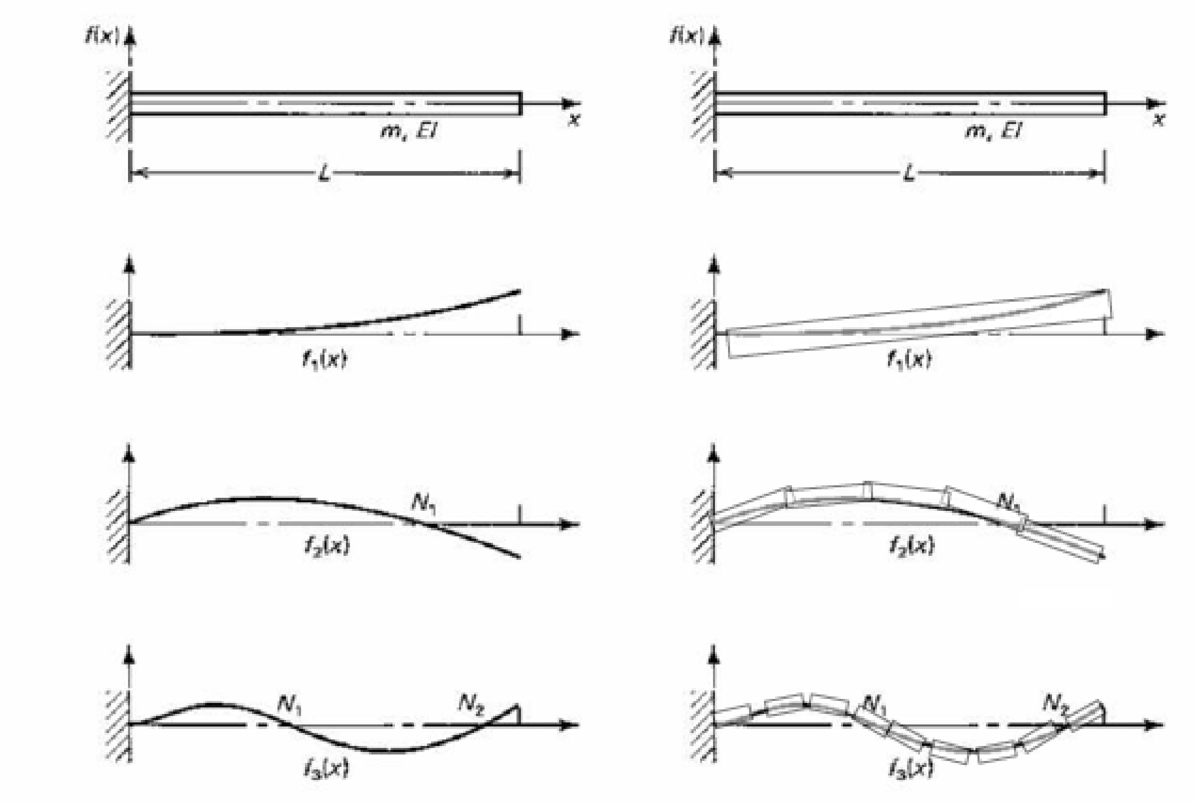

Figure 3-3: example of the shape of the vibrational modes of a clamped/free beam. With on the right a visual representation of how the segments fit these modes. source: Sakshat Virtual Labs website; http://iitg.vlab.co.in/?sub=62&brch=175&sim=1080&cnt=1

considered whether it is of a relevant strength to have an appreciable effect.
A sweep of the literature lead to the following general equation for the energy per area between two walls [14].

$$E_A = -\frac{A_h}{12\pi}\left(\frac{1}{d^2} - \frac{1}{(d+h)^2}\right) \tag{3-15}$$

Where E_A is the energy, d is the distance between the walls, h is the height of the approaching surface and A_h is the Hamaker constant. This constant is in the order of magnitude of ($10^{-19} - 10^{-20}J$, depending on material properties. For our case h is essentially infinite and the equation reduces to

$$E_A = -\frac{A_h}{12\pi}\left(\frac{1}{d^2}\right) \tag{3-16}$$

But with the Hamaker constant being as small as it is this force will negligible in the context of micro systems

3-2-2 Viscous Forces

A possibly more relevant source of damping can be found in the effects of viscosity. The electrode, once brought to vibration, moves inside the liquid it is immersed in and as such will experience effects due to the viscosity of water. More accurately, the hydro-dynamics of the system will possibly affect the damping. This will occur on the side face of the electrode as it moves through the water. In the gap between the electrode and the surface this effect is probably the most pronounced as the viscosity of the liquid between 2 surfaces moving at high frequency in close proximity can be responsible for great damping. intuitively this can be imagined as the "stickyness" experienced once some liquid is placed between for example a piece of plastic and a table. These effects and how they may be modeled are discussed below.

Hydrodynamic damping

First the general effect of hydrodynamics on physical objects in liquid is studied[15], [16]. The most promising method for modeling this behavior in terms of masses and dampers is found in literature [2]. The approximation for the hydrodynamic damping effect is based on the principle of dividing the dynamic effects into an added mass and a damping coefficient. This approximation is based under the assumption that the diameter of the surrounding fluid (environment) divided by the diameter of the cylinder approaches infinity a function H can be defined as follows:

$$H = 1 + \frac{4K_1(\alpha_h)}{\alpha_h K_0(\alpha_h)} \tag{3-17}$$

where K_0 and K_1 are Bessel functions [17] in which α_h is a system parameter which follows from the following equation:

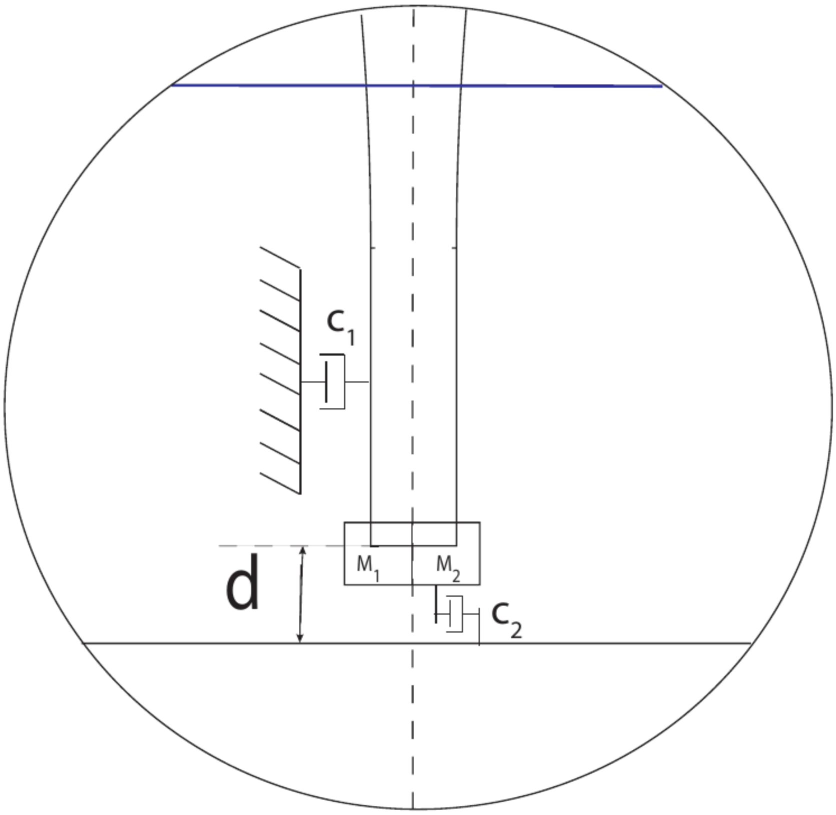

Figure 3-4: Illustration visualizing the damping and added mass principle on the SECM. With C_1 the hydrodynamic damping as defined in 3-1 and C_2 the damping as found in 3-2. the 2 masses are the added masses that are a side effect of these simplifications.

$$\alpha_h = \sqrt{i\frac{\omega}{\nu}}d \tag{3-18}$$

The real part of H represents the added mass C_0 and the imaginary part represents the damping coefficient C_h.

However, it turns out that for the dimensions of the SECM the Bessel functions trend to 0 and this approximation isn't very useful. Therefore the added mass and added damping factor are best determined by reading out from the graphs in [2]. As shown in figure 3-5, where S is a scaled frequency coefficient of the form:

$$S = \frac{\omega d^2}{\nu} \tag{3-19}$$

This won't be very exact, but in fluid dynamics exact results are rarely acquired so experiments to verify model assumptions will be required in any case. Figure 3-4 shows the result of this theory as the damper c_1 and m_1

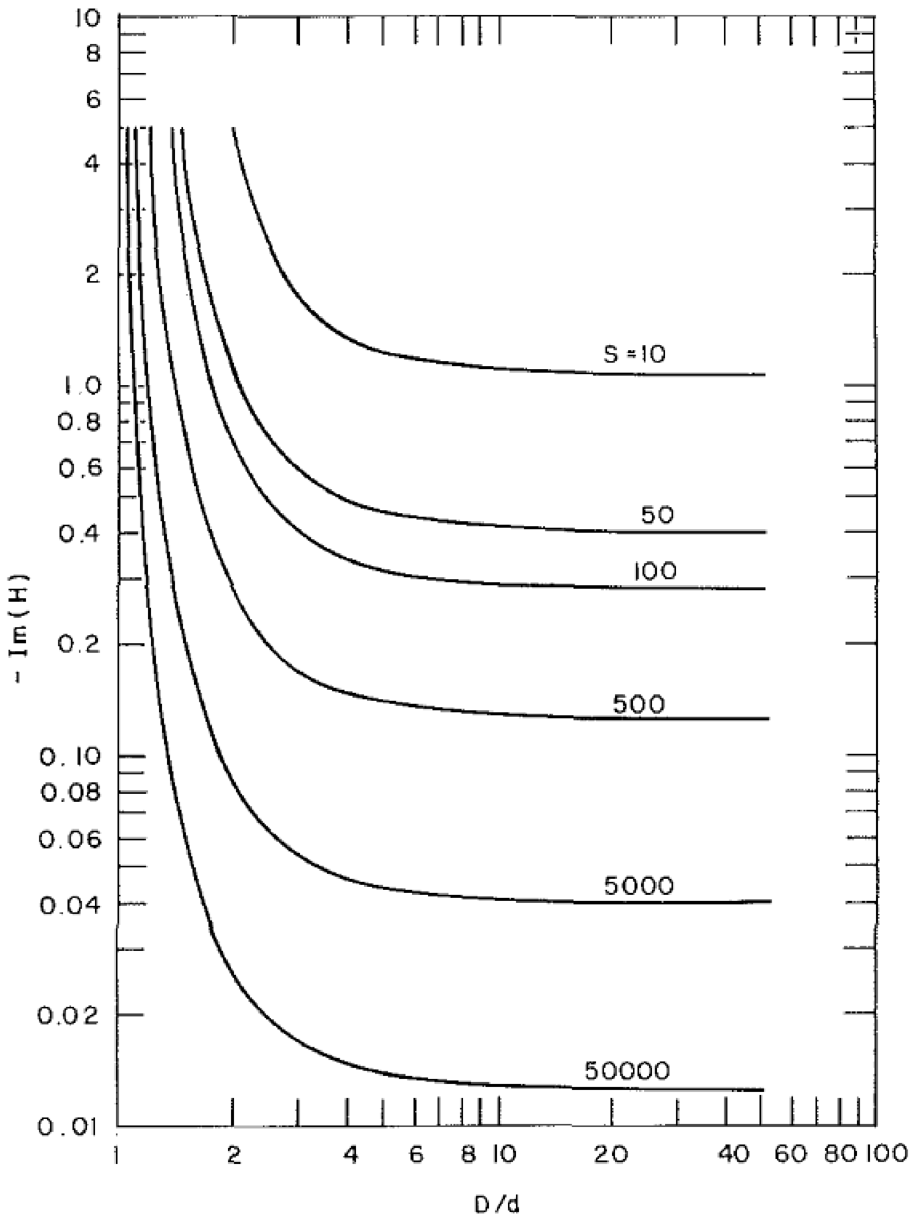

Figure 3-5: Graph for selection of damping coefficient. H being a complex function based on the systems properties described in [2], and S as defined in equation 3-19. D is the size of the surrounding water, d the diameter of the beam.

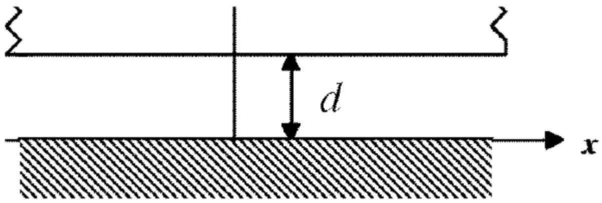

Figure 3-6: Structure of the air-gap. A large surface with an area of A is moving with a velocity of v over a small air gap d. source: [3]

Gap Viscosity Damping

For the gap damping we look at a similar theory but worked out for 2 parallel plates moving past each other [17]. Figure 3-6 illustrates this scenario.

The theory surrounding these calculations takes the following assumptions:

- The amplitude of the oscillation is small compared with the length of the surface.
- The width and length of the surface are large compared with the gap separation.
- The velocity of the surface is low enough to prevent the heating of the gas (or the liquid in our case).

Considering adherence to the assumptions. The first two assumptions are almost certainly met. The final one seems unlikely to be of significant effect in water even for high frequencies. Furthermore, this equation is initially found for a gas, but after discussion an initial assumption (to be tested) is that the incomprehensibility of the liquid won't significantly impact the result for small lateral movement (small angle θ).

The equation governing the lateral speed of the tip v, as seen in the x direction of fig 3-6, boils down to:

$$\frac{\partial v(z)}{\partial t} = \nu \frac{\partial^2 v(z)}{\partial z^2} \tag{3-20}$$

Using function 3-20 the damping admittance is obtained from:

$$\bar{\tau}_{xz} = -\eta A \frac{\partial v(z)}{\partial z}\bigg|_{z=d} \tag{3-21}$$

$$\bar{\xi} = -\frac{\bar{\tau}_{xz}}{v_r} \tag{3-22}$$

Next equation 3-20 needs to be evaluated depending on the boundary conditions. For the continuum (no slip) boundary condition, the final solution for admittance is:

$$\bar{\xi}_0 = \frac{\eta A q}{tanh(qd)} \tag{3-23}$$

with q the complex frequency variable $\sqrt{i\frac{\omega}{\nu}}$

The real part of equation 3-23 is the added damping coefficient for this effect.

figure 3-4 shows this effect included as damper and mass 2.

3-3 System Elements

Aside from the general dynamics of a vibrating beam individual elements of the system will also have to be modeled. These elements require special attention because they have an electrical element and it is important to define how the electrics and structural dynamics relate to each other. The input and output of the system are a voltage and therefor modeling them individually is important..

3-3-1 Lock-in Amplifier

A Lock-In Amplifier (LIA) is an electric device for selecting a very specific and tight frequency band from an input signal. This allows the detection of a frequency specific small amplitude signal from an environment of dominating noise [18]. Essentially amplifying only the content of 1 frequency in a complete signal as seen in figure 3-7

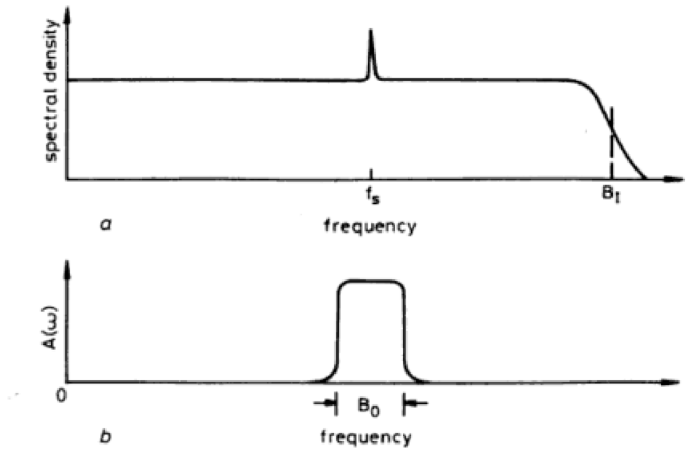

Figure 3-7: A) shows an example signal with the required content at frequency the user is looking to select b) shows the bandpass filter that if applied to the signal of picture a) mirrors the function of a lock-in amplifier.

A specific setup of the LIA called Phase Sensitive Detection (PSD) detects both the amplitude and phase at the selected frequency. What the LIA does is multiply the input signal with a signal of different amplitude and phase:

$$V_{psd} = 0.5V_{sig}V_L sin([\omega_r - \omega_L] + \theta_{sig} - \theta_{ref}) - 0.5V_{sig}V_L sin([\omega_r + \omega_L] + \theta_{sig} + \theta_{ref}) \quad (3\text{-}24)$$

After filtering this signal with a low pass filter only the first section remains, which is equal to zero for all values of ω_L unless it equals ω_r. The resulting output of the PSD is:

$$V_{psd} = 0.5 V_{sig} V_L sin(\theta_{sig} - \theta_{ref}) \tag{3-25}$$

So with prior knowledge of the reference signals amplitude and phase, the amplitude and phase of the input can be found. The application of the LIA in the SECM system used in the experiments is summarized in the diagram in figure 3-8. This figure shows how the inputs are filtered to find Amplitude R and phase shift j.

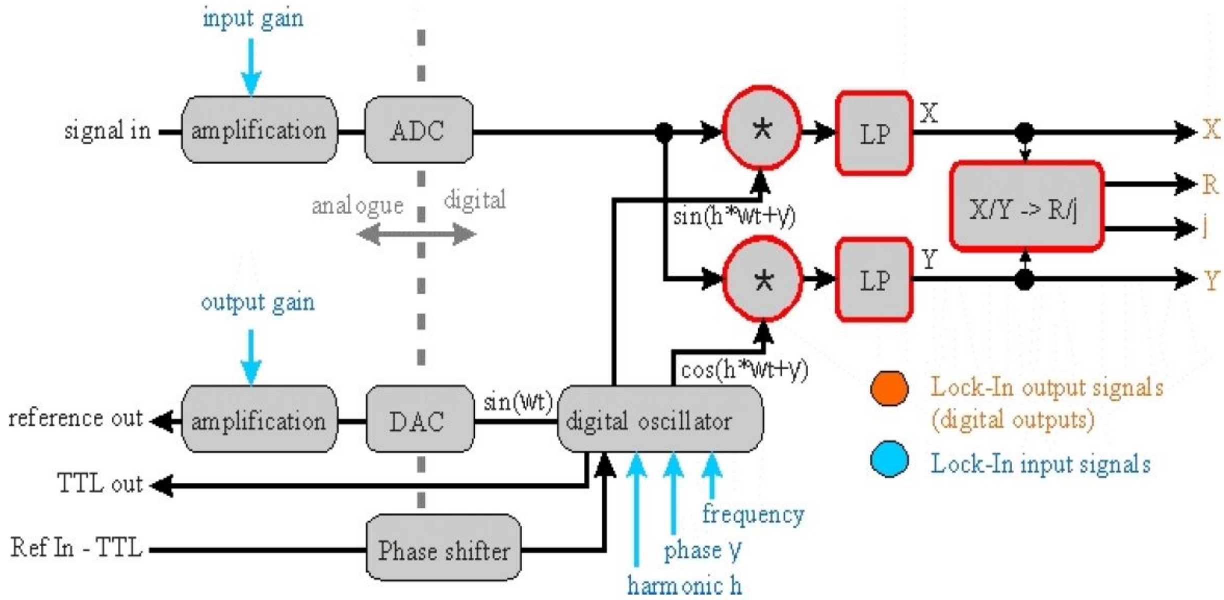

Figure 3-8: This diagram shows all the elements of the LockIn Amplifier as used in the experiments. ADC and DAC are analog to digital converters, LP are Low Pass filters, X contains the real valued output and Y contains the imaginary output. The code used calculates the amplitude and the phase shift from this data. The source of this image is the Lock in Amplifiers manual provided by Sensolytic.

3-3-2 Piezo Crystal Oscillators

This section delves into the piezo-crystal functionality as well as their dynamics. A particular focus is payed to the hysteresis effect.

Piezo basics

Piezo-electric ceramic material will be used for actuation and sensing of the forces in the system. Piezo crystals are widely used in the industry for actuation and precise positioning. Piezo crystals function by the principle of an external potential causing the internal electric dipole moment in a crystalline structure to change, which in turn causes the shape of the material to change (bending or extending depending on crystalinne structure). An example can be seen in figure 3-9. The opposite is also true, the material will generate a voltage upon deformation [4, p.418][19].

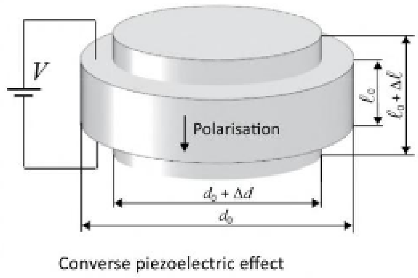

Figure 3-9: Piezo visualisation from [4]

The exact behavior of piezo's is relatively complex. However manufacturers of piezo ceramics provide an approximation between applied voltage and displacement as a simple function:

$$\Delta h = d_{33}U \tag{3-26}$$

Where h is the height of the piezo element, U is the voltage applied and d_{33} is a material constanst for the piezo material.

This type of equation will allow us to build up a dynamic model for the piezo force applied based on Newton's second law:

$$F_{piezo} = m_{piezo}\ddot{x}_{cm} \tag{3-27}$$

where $\ddot{x}_{cm}$ is the acceleration of the center of mass of the piezo element found as the double derivative of the parameter found in 3-26.

Dynamics and hysteresis

In the discussion about the dynamics of piezo crystals, generally the most important factor is considered to be the hysteresis effect [20]. The basic idea of hysteresis is that upon application of a potential the material will have some buildup or discharge time before it changes shape. The most insightful example is imagining a mass moving along a rail attached to a spring. As a force is applied to the spring it will compress a bit before the mass will start moving. Once the force is reversed the spring will have to extend first according to Hooke's law until a new equilibrium is reached. This shows that upon a harmonic excitation at each reversal of the direction of the force a hysteresis effect will appear.
This causes the response to become non-linear with unwanted oscillations and a lack of precision. In extreme cases it can even render systems unstable.

The simplest method for hysteresis prevention is a charge driven approach to piezo actuation[21], [22]. This should greatly decrease the hysteresis effect in the piezo actuator. However if this proves insufficient or other dynamics introduce unacceptable errors a more complex controller might be necessary to compensate.

Controllers have been developed to compensate for the hysteresis effect as well as other local dynamics to have more accurate control over piezo displacement. Basic sensor free controllers are generally Inverse-based Iterative Controllers (IIC) and controllers for the dynamics are based in Iterative Learning Control (ILC) as seen in literature. Some identification of the behavior of the piezos used, is required to create an inverse model and realize feed-forward compensation.
Common model types used in this identification are either the Preisach model or the The Prandtl Ishlinskii model, which serves as somewhat of a simplification of the Preisach model.

3-3-3 Assumptions

All of the theory above leads to a finalized set of assumptions under which the model will labor. These assumptions are summarized here.

1. Point Masses
2. Linear Springs
3. Viscous linear dampers
4. Rigid links
5. Discretization of a continuous beam based on a mass/spring/solid link model [10]
6. Hydrodynamic effect approximated by an added mass and spring.
7. Piezo's are represented as a sinusoidal force initiated by a oscillating point mass
8. Hysteresis effects are negligible

3-4 Discussion

Each individual element of the system has been defined as a function of simple linear elements. All of the assumptions and approximations are made based on rigid scientific research and individually they should all be appropriate and sufficient. The question remains however, whether the combinations of these assumptions are still viable since small errors could carry over and cause problems. Additionally, and more importantly, it remains to be seen whether or not these approximations adequately describe the entirety of the SECM system. It is possible that some dynamic effect was overlooked or that the discretization is too coarse to capture all the relevant behavior. With the high frequency of operation, the size of the micro-electrode element and the degree of manual fabrication the possibilities for these simplifications causing errors should be carefully considered when reviewing modeling results.

Chapter 4

Simulation Results

This chapter will discuss the model implementation in MATLAB. Outlining the used code as well as some mathematical basis for reaching the required algorithm. The results of the final program will also be discussed.

4-1 MATLAB Modeling the Lagrangian System

For modeling the Lagrangian model the same steps taken in the mathematical modeling chapter have to be taken and captured in MATLAB code. The focus of this coding will be on keeping the code as largely parametric as possible. This to allow the code to be ran quickly once variables change. The variables that will be kept parametric are listed in table 4-1

4-1-1 MATLAB Code Description

For the purposes of creating versatile and easily adjustable code each part of the Lagrangian process was set in it's own function. The functions used are described below.

LoadPar and LoadPPar

These codes contain the symbolic parameters in `Par` and the used values in `PPar`. This will ensure that a changed parameter is applied throughout the code as well as making substitution easier and less error prone.

Kinematic and Symbolic

The kinematic function expresses the movement and speed in the x and y direction of each segment as a function of the appropriate angles θ and those variables kept symbolic with PPar. Symbolic then creates a completely symbolic set of directions x and y as well as their speeds and acceleration which are used to create the vectors with generalized coordinates, generalized velocities and generalized accelerations. Named q, qd and qdd respectively.

Table 4-1: Variables for experimentation with SECM model

Variable	Physical meaning	Use in modeling
`n`	Number of Segments	This value will allow the user to adjust the discretization of the tip.
`E`	The Youngs Modulus of the Glass	This factor is responsible for the spring constants involved. Since it is one of the crudest simplifications in the model, adjusting it to fit the model to the experimental data might be required.
`cg`	the Gap damping	The damping introduced by a beam in liquid near a surface.
`ch`	the Hydrodynamic damping	The damping introduced by the hydrodynamic effect of a beam vibrating in liquid.
`cseg`	Individual Segment damping	The damping added to each segment as an additional measure to allow for better fitting, and possible correct for oversimplified assumptions.

Masses
`ma`
`m1 m2`
`ms`
	
	The Added Masses due to Damping
	The Mass of the Brass Holders
	Mass of individual segments
		
		Keeping them variable would be preferred
		but due to reasons explained later this was not
		possible.

$$\mathbf{M} = \frac{\partial EOM}{\partial \mathbf{qdd}} \quad (4\text{-}1) \qquad \mathbf{C} = \frac{\partial EOM}{\partial \mathbf{qd}} \quad (4\text{-}2) \qquad \mathbf{K} = \frac{\partial EOM}{\partial \mathbf{q}} \quad (4\text{-}3)$$

Energies

The energies function defines the Potential, Kinematic and non-Conservative forces as a function of the generalized coordinates. For clarity each source of energy is defined and totaled seperatly after which they are combined into one.

Lagrangian

Lagrangian simply calculates the Lagrangian and finds the equations of motion for the system as a function of the generalized coordinates and the variables that are kept symbolic. The mathematical basis for this is found in chapter 3.

Linearization and the State space form

The remainder of the code as can be seen in the appendix will generate Mass Matrix $\mathbf{M}$, Coriolis matrix $\mathbf{C}$ and Stiffness matrix $\mathbf{K}$. This by individually partially differentiating the full equation of motion towards the generalized accelerations, velocities and positions respectively. As illustrated in equation 4-1 through 4-3

The system is then generated by lineraizing these matrices around $\theta = 0$. Using these linear system matrices the system:

$$\mathbf{M}\ddot{\theta} = -\mathbf{C}\dot{\theta} - \mathbf{K}\theta \tag{4-4}$$

was transformed to create the state space

$$\begin{bmatrix} \dot{\theta} \\ \ddot{\theta} \end{bmatrix} = \begin{bmatrix} 0 & \mathbf{I} \\ \frac{-\mathbf{K}}{\mathbf{M}} & \frac{-\mathbf{C}}{\mathbf{M}} \end{bmatrix} \begin{bmatrix} \theta \\ \dot{\theta} \end{bmatrix} + \mathbf{Bu} \tag{4-5}$$

Attempts were made here to generate a symbolic mass matrix. However in order to generate the state space system the mass matrix needs to be inverted. Inverting a symbolic matrix proves very difficult for MATLAB. Upon experimentation only matrices upto 5 segments provided invert-able mass matrices. Five segments is far to few to provide useful results and we were forced to consider systems with all masses as set constants. The only possibility of varying the masses for testing is to create a set of matrices based on different mass settings and compare results based on individual simulations for said systems.

Sysgeneration and Frequency sweep

Sysgeneration is simply a combination of the codes outlined above intended to generate a state space system with the required elements kept variable for simulation. $Frequencysweep$ then uses the system created by sysgeneration in order to simulate the same type of frequency sweep as was preformed during the experiments as outlined in chapter 2. For this purpose we need to gather the amplitude outcomes for a range of frequencies. The bode plot should prove useful for achieving this goal.
A problem with using the bode plot is that it is supplied with a sample of frequency points that is generated based around optimizing the speed of the algorithm. These points are rarely the same and the number usually isn't even the same making comparison to the experimental data impossible. It is also possible to feed the bode function a user generated sample vector. Using this function a logarithmic vector was created containing a set number of values between 100 kHz and 400 kHz. This same vector was then used for the sampling of the experiment data of the frequency sweeps. One final step that had to be taken was to ensure the same units were used. The bode plot operates in radians per second and the experiment was carried out in Hz. Therefor the input vector of the bode function was scaled to also be expressed in Hz. As such 2 vectors of amplitude values sampled at the same frequencies were created.

4-1-2 Parameter effects

While playing with the outcome of the simulation 2 primary effects where noticed. Adjusting E would move the plot along the x-axis. Basically taking roughly the same shape of graph and moving it along the frequency spectrum.
The effect of cseg was intuitive, it flattened all the resonance peaks. Results of these simulations are illustrated in figure 4-1 for the variation of E and in figure 4-2 for the variation of cseg. For the variation of cseg it is important to note that the stated values are based on a scaling used for optimization. The actual in model value used is found by taking the noted value of cseg and entering into equation 4-6, E is simply scaled by a factor of 10^{-2} in this case.

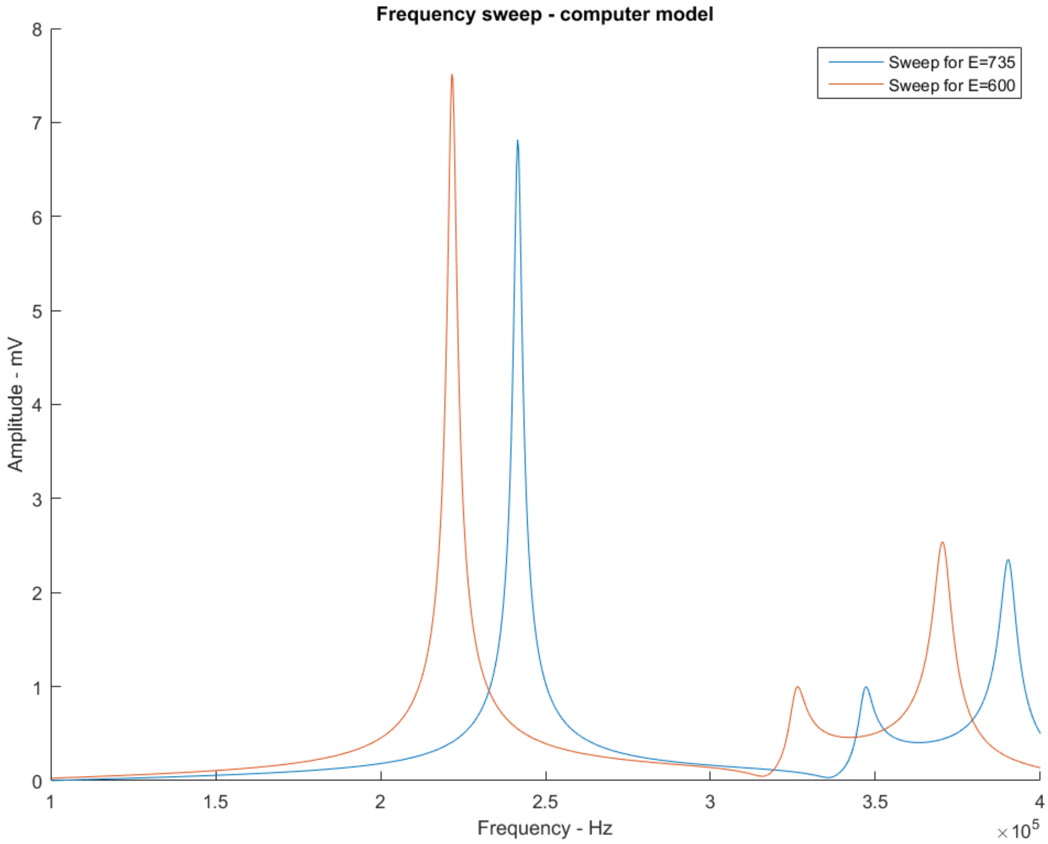

Figure 4-1: A couple of Frequency sweeps showing the effect of changing the Young's modulus E. With increasing E the peaks move to the right along the x-axis. E is scaled with a factor $\frac{1}{100}$ for the sake of the optimization algorithm.

$$damping = \frac{1}{cseg} 10^{-6} \tag{4-6}$$

Number of Segments

The number of segments also has a clear effect. The initial number of segments selected was 29, based on the theory discussed in chapter 3. Changing the number of segments to another number creates a radically different shape but doesn't introduce a more rich or diverse behavior, as seen in the non optimized frequency sweep graph of figure 4-3. As such future research using this approach would not require a very large number of segments. However due to the consistency in regards to the assumptions made earlier in the discussion of vibration modes this research will try to stick to the larger numbers as stated above. An additional advantage of a large number of segments is that it allows for easily and precisely changing the position of in- and outputs in the state space model, adding to the models versatility. With the glass tips changing often and have different behavior such versatility is valuable.

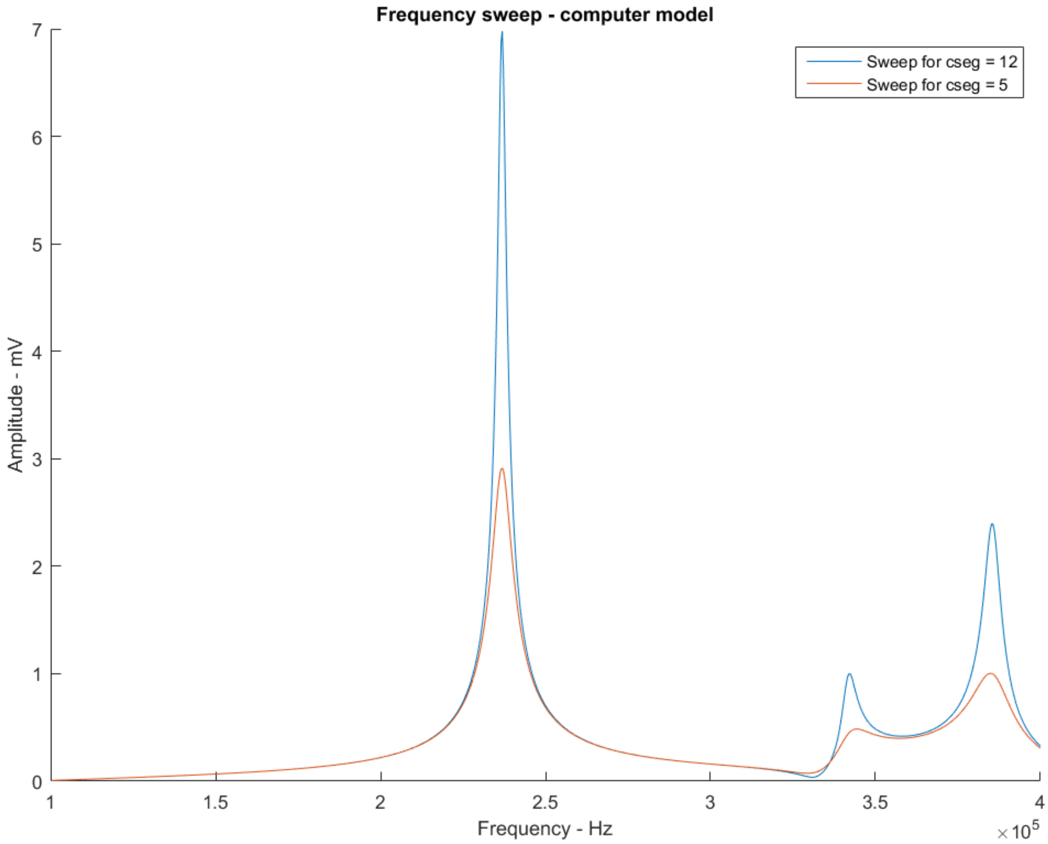

Figure 4-2: A couple of Frequency sweeps showing the effect of changing cseg. With increased damping the peaks are attenuated. note: for optimization reasons the value of cseg are scaled. $\frac{1}{cseg}10^{-6}$ results in the actual value used.

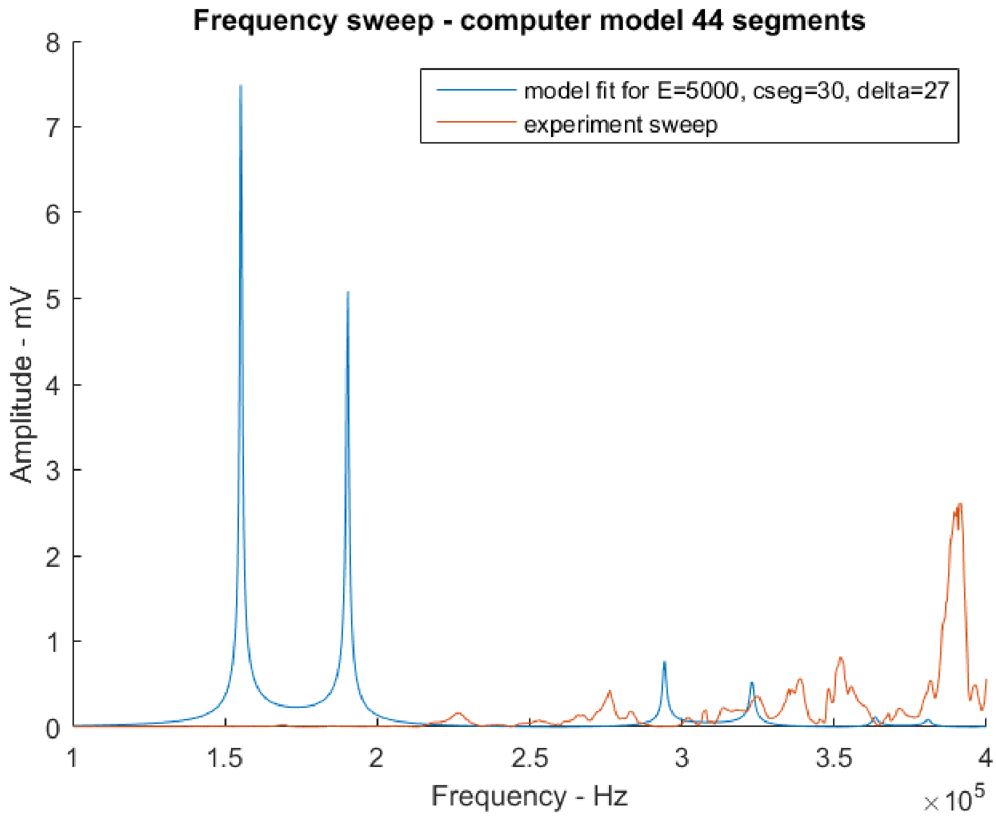

Figure 4-3: A frequency sweep graph of the model compared to a sample experiment sweep. Used number of segments is 10. The behavior is similar enough to suggest lower numbers of segments is not detrimental to the results. It does however not show any significant improvement over higher segmented models.

Below 8 segments the frequency behavior in the range interesting to this research disappears so anything under that threshold is not relevant for study.

4-2 Optimization Fitting

The final step to test if the created model was able to capture the required behavior was to write an optimization algorithm. The purpose of this algorithm was to compare the experiment data with the model data and minimize the difference.

The function of the frequency sweep is highly non-linear and non-convex. On top of that many steep local minima are to be expected. With peaks unaligned the difference can be very large where only a slight shift can create a much better fit. Finally, as mentioned before, the mass matrix couldn't be kept symbolic. And if it needed be varied a discrete set of mass matrices would have to be created and sampled to test for the best result. For these reasons the very general purpose genetic algorithm was chosen. It is able to tackle almost any function and the MATLAB version can rather easily include discrete parameters as part of the optimization. The algorithm would then have to be ran a couple of times in order to avoid the effect of local minima. The used variables for the initial optimization are seen in table

4-2. Delta in this table is a factor intended for linear scaling to bring the values of the model and the experiment in the same order of magnitude. The mass is not included in this for the reasons stated earlier. Finally all these variables where scaled such that they all fell into the 0-1000 range. The scaling is also noted in the table.

The first and important observation is that taking the estimates for the variables based on the physics discussed in chapter 3 does not result in a reasonable fit. The conclusion is that due to the many approximations these values will have to be set in a more abstract manner. This is an unfortunate departure from the stated goals of keeping the model rooted in physical reality but the hope is that based on the experience of the effect of these values we are still able to adjust them fairly easily to fit a new situation in practice. In other words, after changing tips new optimization could still be quick because of initial guess of the parameters.

Table 4-2: Variables for optimization of the SECM model

Variable	range	scaling factor
`E`	0-10000	$\frac{E}{100}$
`delta`	0- inf	$delta \cdot 10$
`cseg`	10^{-9}- 10^{-6}	$\frac{1}{cseg}10^{-6}$
`mi`	$10 - 10^{-4}$	no scaling, list provided

Fit Results

The result of the optimization shows a reasonable fit of the high frequency segment is possible. The result of this fit is shown in figure 4-4. It becomes readily apparent though, that the lower frequency peak around 250 kHz pretty much invalidates the fit. Unfortunately no better fit was found. Some gave a better fitness overall but non approached the curve to an acceptable degree.

Fits with different numbers of segments where attempted. Possibly even more segments where required to fit the behavior well. One of the better results of this fit is displayed in figure 4-5. The problem of the low frequency peak is supressed, but it is still present. At high frequency the behavior for the highest peak seems pretty good but the fit for secondary peaks in that region is lost. The higher number of segments didn't solve the problem to satisfaction.

4-3 Discussion

This Chapter discusses the way the model was constructed and how it behaved in simulation. The model showed the type of behavior that is expected of a vibrating beam. The model is very versatile, changing the number of segments in combination with the spring and damping constants allows for a large degree of customization. Unfortunately, while the model can partially fit to the data generated by physical experiments, the results miss some of the added

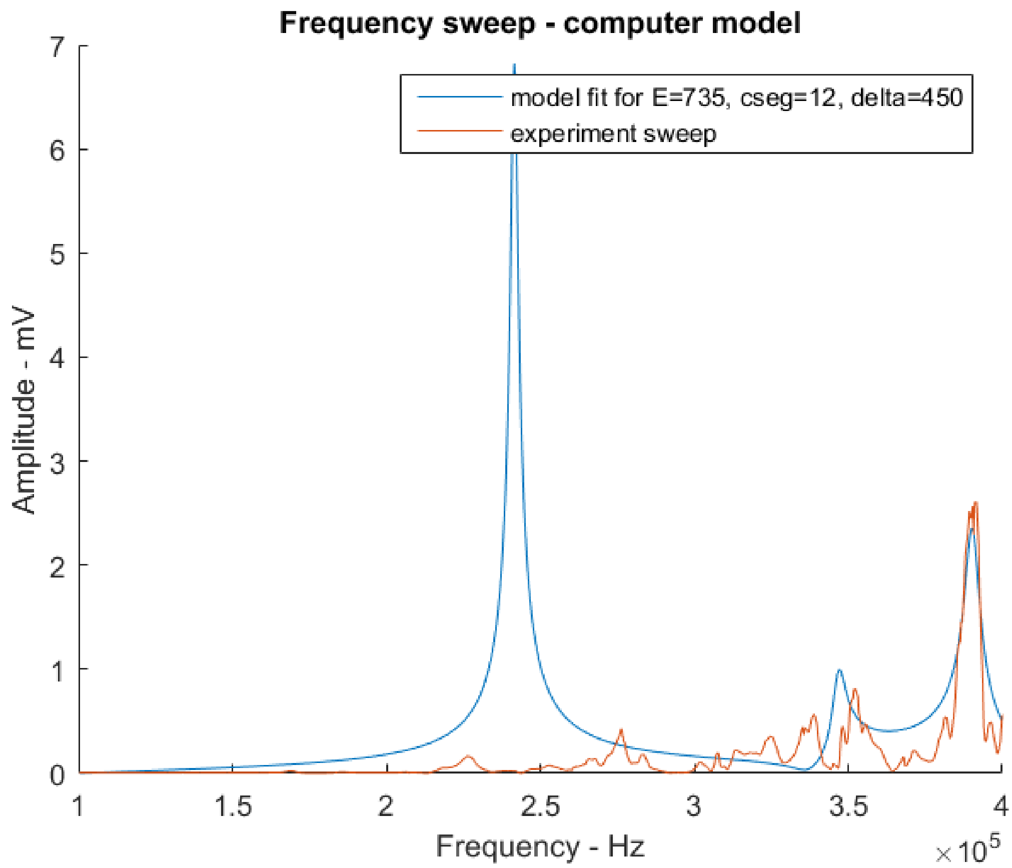

Figure 4-4: A fit of the model to the experimental data. A reasonable fit for the peaks in the 300 to 400 kHz range is achieved but a very sharp additional peak in the lower range causes significant problems.

dynamic behavior seen in lower frequencies. Being a linear model based on approximations it also doesn't show much of the noise seen in the experiments. This should not prevent a good fit under normal conditions, but for the intended operation of the device the amplitude/frequency relation has to be known to a very exact degree for both the damped and the un-damped case. Any controller based on this model would be very susceptible to these noisy peaks in the behavior because even relatively small (0-10 %) errors mistakenly identify the current position as being in the Shear Force region. Due to the lack of precision in the beam dynamics model it is very difficult to make definitive claims about the precision of the damping assumptions. With the results of added mass and damping changing the output, but the lack of fitness of the original model making comparisons to the changes as seen in the experiments difficult.

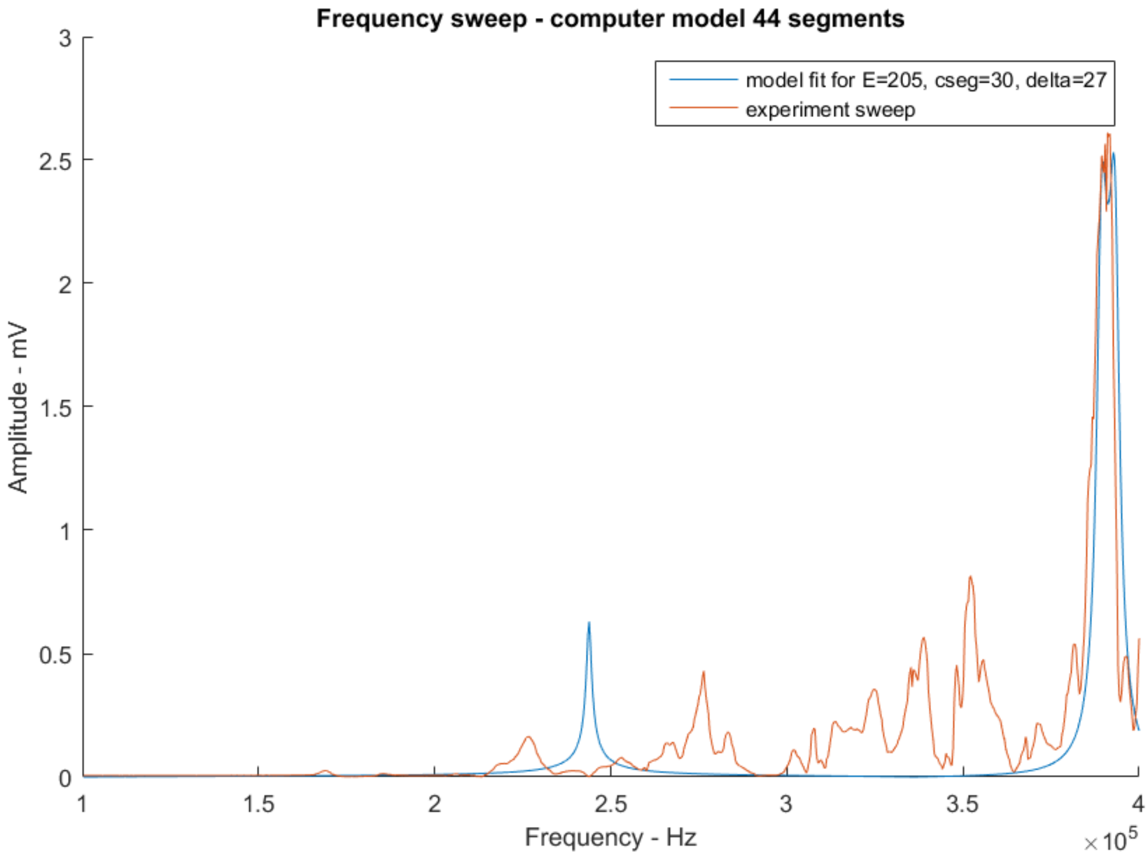

Figure 4-5: A fit of the model to the experimental data. A 44 segment model can create a peak with a more suppressed low frequency problem but it is still present and we loose some of the high frequency fit in the secondary peak.

Chapter 5

Discussion and Suggestions

This section Discusses the result of the research and finally adds some suggestions on how future research might build upon it to reach new and possibly better results.

5-1 Discussion

The conclusion has to be that the chosen modeling approach does not provide a model of the required quality. Most of the attempts contained too many inaccuracies to be used as a full model of the Scanning ElectroChemical Microscopy (SECM) system. At 29 segments a section of the behavior is approached but with a large section of the graph acquired from the experiment being completely absent from model simulation can't be used for any model based control approach. Increasing or decreasing the numbers of segments didn't provide any appreciable benefit. This suggests that a discritized model will always have problems to capture the behavior well.
Looking at the smoothness of the curves it seems very unlikely that this type of model would ever come close enough to the curves seen in the experiments. Additionally, it is difficult to say if the damping method of added damping and added mass works, although looking at all the existing literature it is essentially they only available option that isn't based in large equations based around the Navier-Stokes equations.
Looking critically at the experimental data however, it should be possible to match all the resonance peaks. But matching the exact noisy peaks on the smaller scale seems increasingly unlikely. This behavior varies from run to run with varying conditions. Little particles in the liquid and stick slip phenomena near when the tip comes within the nano meter range are likely candidates for this type of behavior. Additionally it was observed that even small disturbances of the table on which the system is placed will give a noticeable disturbance of the output system. While this can be prevented in laboratory conditions, in the industry a model based on this lack of disturbance would not suffice. Based on these observations a more model free approach, or at least one that doesn't cover the entire frequency range, will have to be seriously considered.

Here the posed research questions are addressed.

- *"Can a series of experiments be devised that will sufficiently show the required dynamic behavior of the system?"*

  The experiments provided a wealth of data and experience with the system. The current data set should prove very useful for future modeling and expanding upon the experiments in the future should be relatively simple using the required expertise.

- *"Is it possible to model the SECM system in an analytic manner?"*
  "Is it possible to clearly identify the systems real world parameters in the model?."

  This has proven very difficult. Some essential section of the dynamics can be approached reasonably but a significant amount of the behavior is left out. As such the model was not as precise as was required.

- *"Can a high precision constant distance controller be synthesized using the model?"*

  At this point the model is not sufficient to develop such a controller.

Taking all this in consideration the main question:

"Is it possible to model the SECM system in such a way that positioning control can be improved, and with it the quality of images acquired?"

Must be answered by:

"Not under the current approximations and assumptions. Further research into modeling this system is required."

5-2 Suggestions for Future Research

5-2-1 Model Improvements

A few possibilities come to mind in regards to improving the current model. It might be possible to create the model with the type of diversity required by making each element of the tip individually defined. This would mean each would have a unique spring and damping element. The non-homogeneous nature of the tip might be beter modeled in this way. It would make the model extremely computationally intensive but some exploration into the effect of variations among the parameters would quickly show if such an approach is likely to yield significant improvements.

A second attempt might focus on finding a different initial approximation of the behavior of a flexibel beam. This assumption lies at the hearth of the current model and a if a different method exists it should be relatively simple to adjust the existing code to function for such a new approximation.

A more brute force black box identification of the experiment frequency sweep plots could yield a good fit. However as stated in the report such an approach seems unwise since tips are rotated frequently and based on the experimentation such a new tip would likely force a complete new identification. Making such an effort unlikely to be worth the hassle.

5-2-2 Promising Research Options

Testing whether or not the damping assumption as stated in this report is correct could prove really valuable. Perhaps by building a custom setup specifically geared towards testing this effect. It seems likely that some kind of solution for the general dynamics can eventually be found. But this hydrodynamic damping will always be a bottleneck for a full system model of the SECM.

In terms of the control of the system it might be worth while to look at ways to improve the current control scheme while forgoing the modeling of the system as a whole. Once a frequency of operation is chosen this actuation frequency doesn't change during the control action. With it the initial amplitude and the Shear Force damped amplitude are also locked. As observed, these values don't change as long as the system is left undisturbed.
Using this knowledge in combination with the shape of the approach curves it might be possible to build some type of controller that uses prior knowledge of the initial amplitude value and the final amplitude value in combination with the known shape of the approach curve. This could be used to build a more complex reference tracker initiated by the output exceeding certain bounds around the initial value. After this trigger an appropriate reference signal would then be tracked allowing for online tracking without pre positioning the tip. An illustration of this is shown in figure 5-1. The goal of such a controller would be to keep the X position in the middle of the curve. In the case of the illustration around the 11.5 mV value.

In terms of research that might be of interest once a successful model or control strategy has been achieved. It has been noted that the SECM system runs into problem once it approaches sharp edges in topography. At such an edge the image resolution temporarily breaks down as the Shear Force detection doesn't kick in until the tip has already come really close to the rising or falling edge. An interesting challenge would be to think of a way to predict and anticipate such edges. Is there a detectable signal that could be used to improve behavior in these regions by initialing the reference tracking earlier and keep the distance constant more consistently.

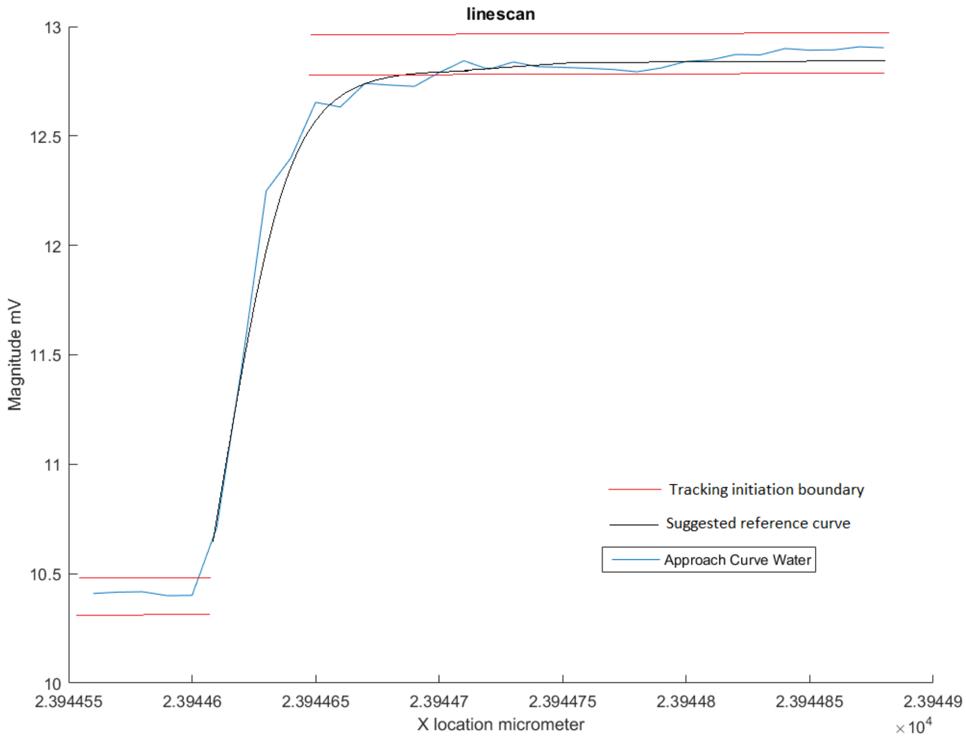

Figure 5-1: This illustration shows an approach curve obtained from the experiments. In black is a possible reference system that would allow a controller the follow this curve. In red are boundaries that once crossed could trigger the start of said tracking.

Appendix A

Additional Frequency Sweep Graphs

A-1 Appendix A - Additional Graphs

A-1-1 Day 1

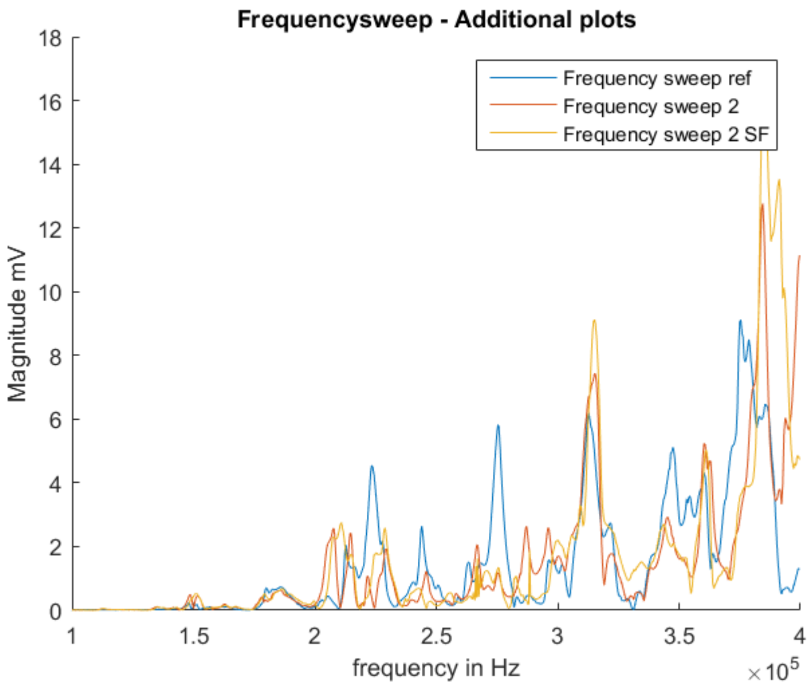

Figure A-1: Frequency sweep response, showing a reference run a run in bulk and a run in the SF range.

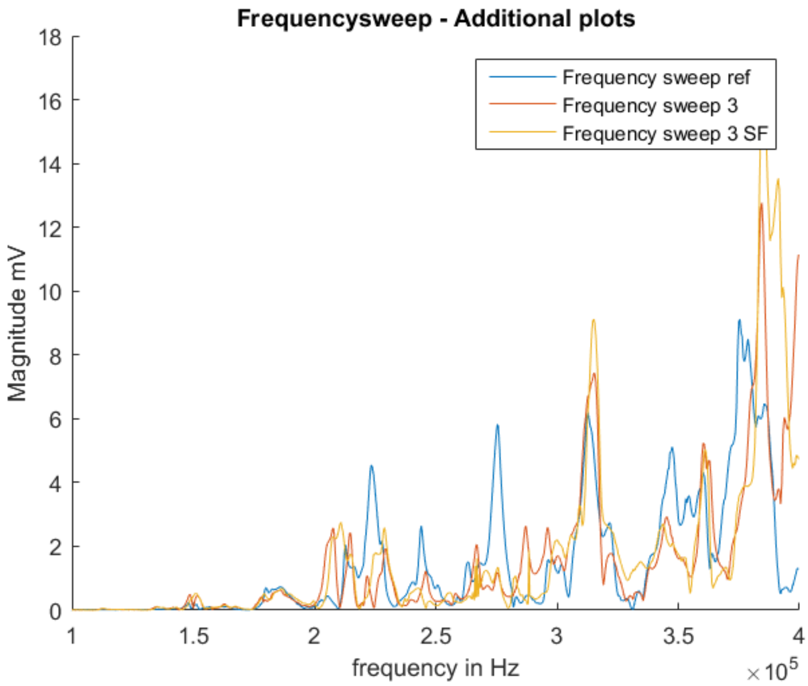

Figure A-2: Frequency sweep response, showing a reference run a run in bulk and a run in the SF range.

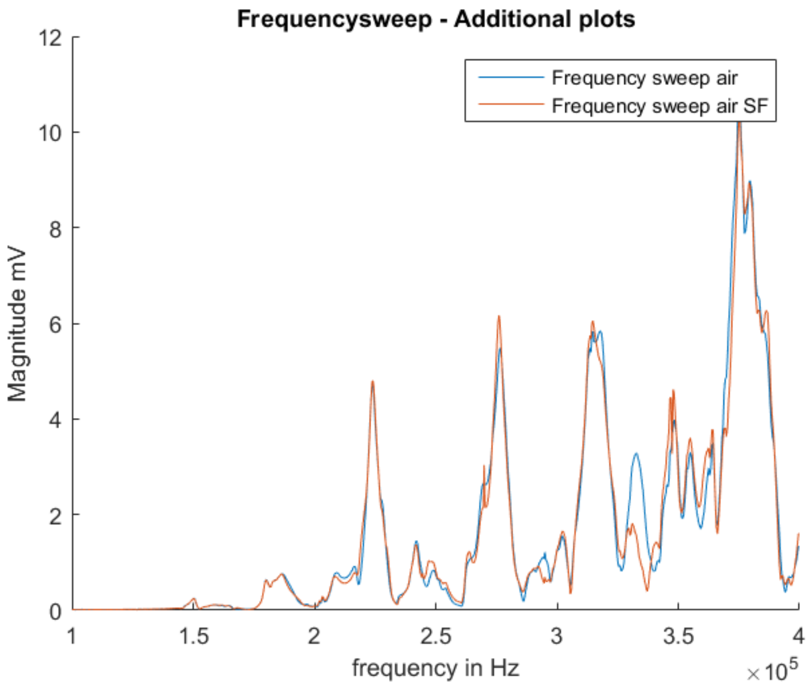

Figure A-3: Frequency sweep response for water, showing a run in bulk and a run in the SF range.

A-1-2 Day 2

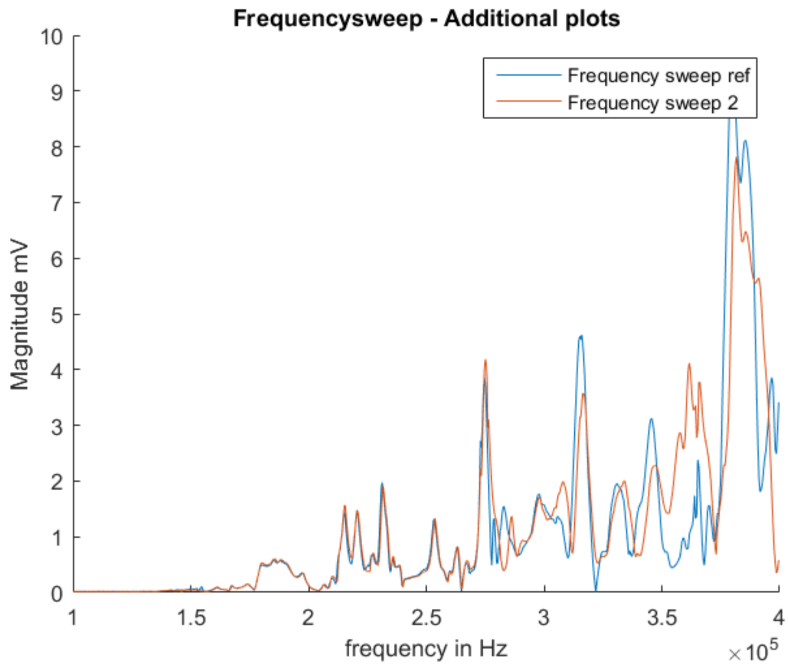

Figure A-4: Frequency sweep response, showing a reference run a run in bulk and a run in the SF range.

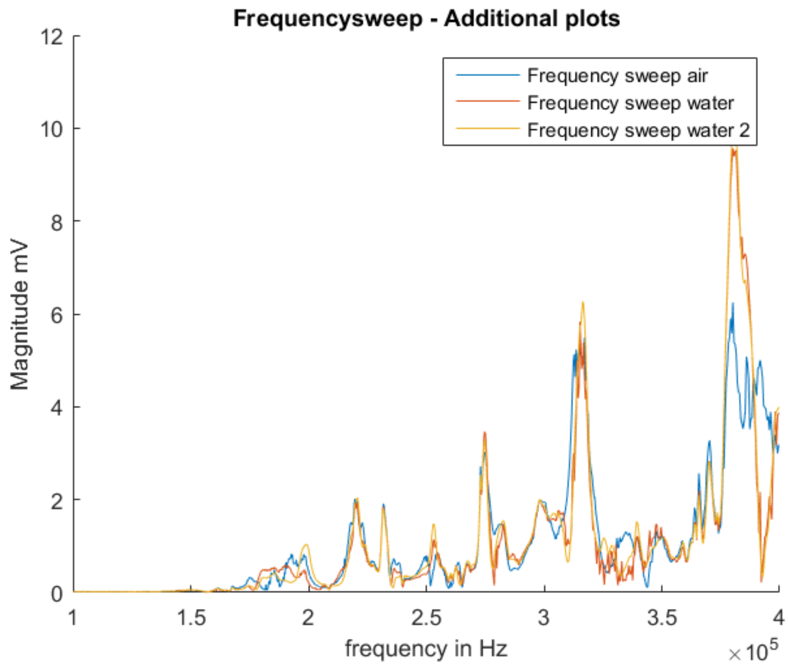

Figure A-5: Frequency sweep response, showing a reference run a run in bulk and a run in the SF range.

A-1-3 Day 3

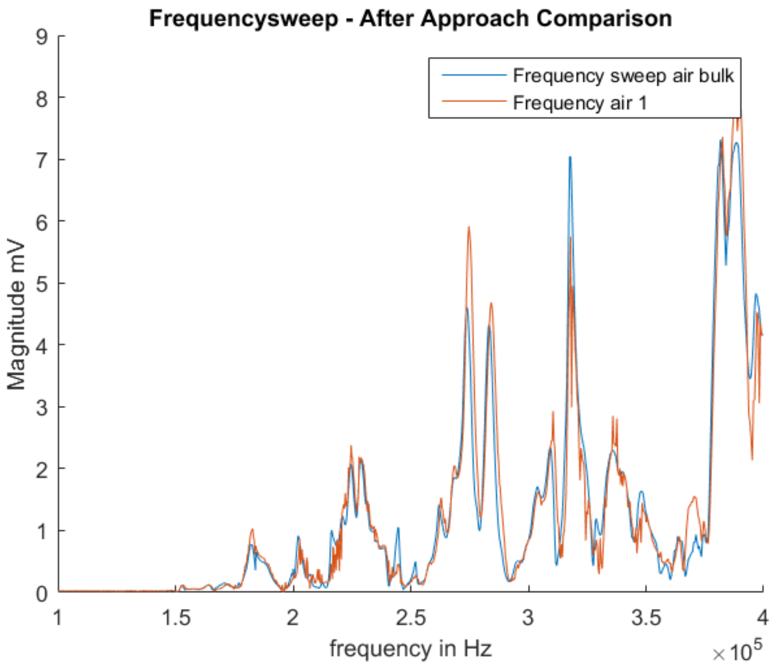

Figure A-6: A frequency sweep in water, comparing bulk vs approach towards the surface responses. Run 1

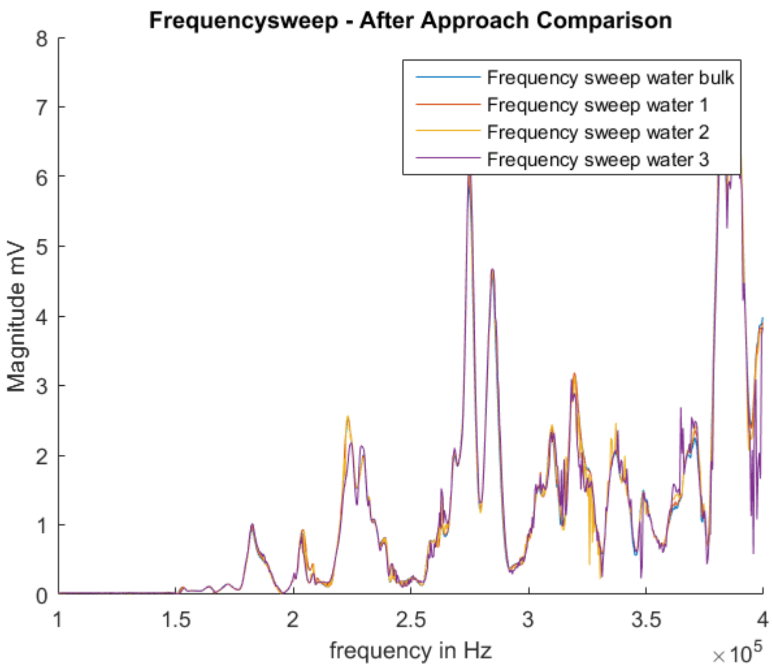

Figure A-7: Frequency sweep in air, comparing bulk vs approach towards the surface responses. Run 1

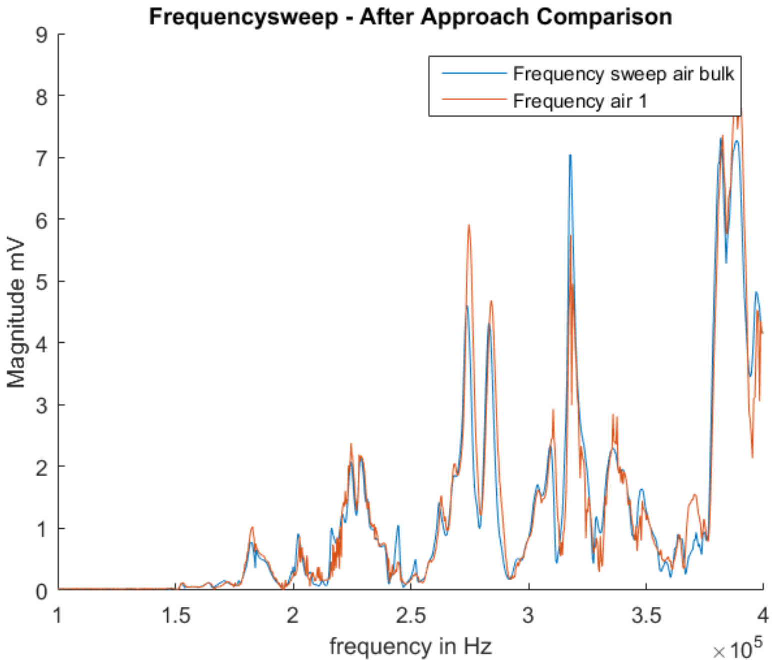

Figure A-8: Frequency sweep in water, comparing bulk vs approach towards the surface responses. Run 2

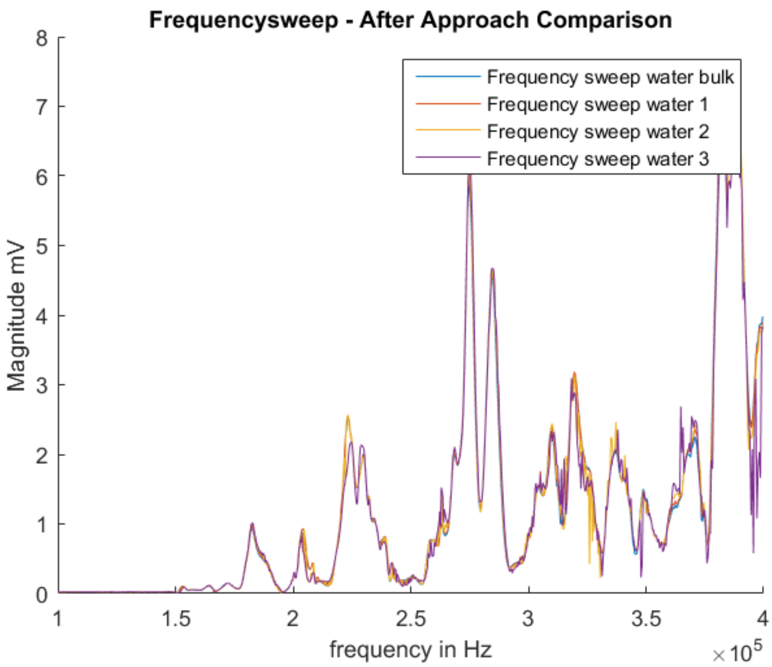

Figure A-9: Frequency sweep in air, comparing bulk vs approach towards the surface responses. Run 3

Bibliography

[1] M. K. Ghatkesar, T. Braun, V. Barwich, J.-P. Ramseyer, C. Gerber, M. Hegner, and H. P. Lang, "Resonating modes of vibrating microcantilevers in liquid," *Applied Physics Letters*, vol. 92, no. 4, p. 043106, 2008.

[2] S. Chen, M. t. Wambsganss, and J. Jendrzejczyk, "Added mass and damping of a vibrating rod in confined viscous fluids," *Journal of Applied Mechanics*, vol. 43, no. 2, pp. 325–329, 1976.

[3] T. Veijola and M. Turowski, "Compact damping models for laterally moving microstructures with gas-rarefaction effects," *Microelectromechanical Systems, Journal of*, vol. 10, no. 2, pp. 263–273, 2001.

[4] R. M. Schmidt, G. Schitter, and A. Rankers, *The Design of High Performance Mechatronics-: High-Tech Functionality by Multidisciplinary System Integration.* IOS Press, 2014.

[5] P. Sun, F. O. Laforge, and M. V. Mirkin, "Scanning electrochemical microscopy in the 21st century," *Physical Chemistry Chemical Physics*, vol. 9, no. 7, pp. 802–823, 2007.

[6] M. Gebala, W. Schuhmann, and F. La Mantia, "A new ac-secm mode on the way to high-resolution local impedance measurements in secm," *Electrochemistry communications*, vol. 13, no. 7, pp. 689–693, 2011.

[7] B. Ballesteros Katemann, A. Schulte, and W. Schuhmann, "Constant-distance mode scanning electrochemical microscopy (secm)âĂŤpart i: Adaptation of a non-optical shear-force-based positioning mode for secm tips," *Chemistry–A European Journal*, vol. 9, no. 9, pp. 2025–2033, 2003.

[8] B. Ballesteros Katemann, A. Schulte, and W. Schuhmann, "Constant-distance mode scanning electrochemical microscopy. part ii: High-resolution secm imaging employing pt nanoelectrodes as miniaturized scanning probes," *Electroanalysis*, vol. 16, no. 1-2, pp. 60–65, 2004.

[9] E. M. H. Amine, "Visualization of local biocatalytic activity using scanning electrochemical microscopy," *Bochum, Bochum, Germany*, p. 120, 2008.

[10] S. S. Rao and F. F. Yap, *Mechanical vibrations*, vol. 4. Addison-Wesley New York, 1995.

[11] J. Hutchinson, "Transverse vibrations of beams, exact versus approximate solutions," *Journal of Applied Mechanics*, vol. 48, no. 4, pp. 923–928, 1981.

[12] J. H. Ginsberg, *Advanced engineering dynamics.* Cambridge University Press, 1998.

[13] M. Liu and D. Gorman, "Formulation of rayleigh damping and its extensions," *Computers & structures*, vol. 57, no. 2, pp. 277–285, 1995.

[14] R. Tadmor, "The london-van der waals interaction energy between objects of various geometries," *Journal of Physics: Condensed Matter*, vol. 13, no. 9, p. L195, 2001.

[15] C. Vančura, I. Dufour, S. M. Heinrich, F. Josse, and A. Hierlemann, "Analysis of resonating microcantilevers operating in a viscous liquid environment," *Sensors and Actuators A: Physical*, vol. 141, no. 1, pp. 43–51, 2008.

[16] T. Naik, E. K. Longmire, and S. C. Mantell, "Dynamic response of a cantilever in liquid near a solid wall," *Sensors and Actuators A: physical*, vol. 102, no. 3, pp. 240–254, 2003.

[17] S. Kirstein, M. Mertesdorf, and M. Schönhoff, "The influence of a viscous fluid on the vibration dynamics of scanning near-field optical microscopy fiber probes and atomic force microscopy cantilevers," *Journal of Applied Physics*, vol. 84, no. 4, pp. 1782–1790, 1998.

[18] M. L. Meade, *Lock-in amplifiers: principles and applications.* No. 1, Mike Meade, 1983.

[19] B. Jaffe, *Piezoelectric ceramics*, vol. 3. Elsevier, 2012.

[20] D. Croft, G. Shed, and S. Devasia, "Creep, hysteresis, and vibration compensation for piezoactuators: atomic force microscopy application," *Journal of Dynamic Systems, Measurement, and Control*, vol. 123, no. 1, pp. 35–43, 2001.

[21] S. Lining, R. Changhai, R. Weibin, C. Liguo, and K. Minxiu, "Tracking control of piezoelectric actuator based on a new mathematical model," *Journal of Micromechanics and Microengineering*, vol. 14, no. 11, p. 1439, 2004.

[22] Y. Wu and Q. Zou, "Iterative control approach to compensate for both the hysteresis and the dynamics effects of piezo actuators," *IEEE Transactions on Control Systems Technology*, vol. 15, no. 5, pp. 936–944, 2007.

Glossary

List of Acronyms

DCSC	Delft Center for Systems and Control
MSE	Material Science Engineering
SECM	Scanning ElectroChemical Microscopy
AFM	Atomic Force Microscopy
FEM	Finite Element Modeling
IIC	Inverse-based Iterative Controllers
ILC	Iterative Learning Control
LIA	Lock-In Amplifier
PSD	Phase Sensitive Detection
SF	Shear Force

List of Symbols

α	Angle between piezo sensor and actuator
F	Faradays constant
Co	Concentration of electro-active species
Di	Figgustion Coefficient
r	radius
a_i	length in SECM micro-electrode tip
F_i	Force in SECM micro-electrode tip
Ah	Hamakers constant
H	Function used in hydrodynamic damping calculation
K_0	0th Bessel function
K_1	1st Bessel function
α_h	System parameter for hydrodynamic damping modeling
C_0	Added mass element of H equation
C_h	Added damping element of the H equation
ν	Kinematic Viscosity
d_{33}	Piezo crystal material constant
d	distance between micro-electrode and substrate surface
θ	angle of rotation of SECM in relation to the y-axis
ω	Frequency of excitation
V	Potential Energy
T	Kinetic Energy
R	Non-Conservative Force
ρ	Density
A	Surface area
E	Young's Modulus
I	Moment of Inertia
Re	Rayleigh's quotient
n	number of tip elements
q_i	Generalized model coordiantes
k_i	Spring constant
c_i	General damping coefficient
c_{seg}	Tip segment damping coefficient
c_h	Hydrodynamic added damping coefficient
c_g	Gap added damping coefficient
m_1	Mass of the piezo actuator
m_2	Mass of the piezo sensor
m_s	Mass of a individual tip segment element
m_a	Mass representative of the added damping
K	Elasticity Matrix
C	Coriolis Matrix
M	Mass Matrix